STABLE LASER SOURCES FOR THE FORMATION OF ULTRACOLD MOLECULES

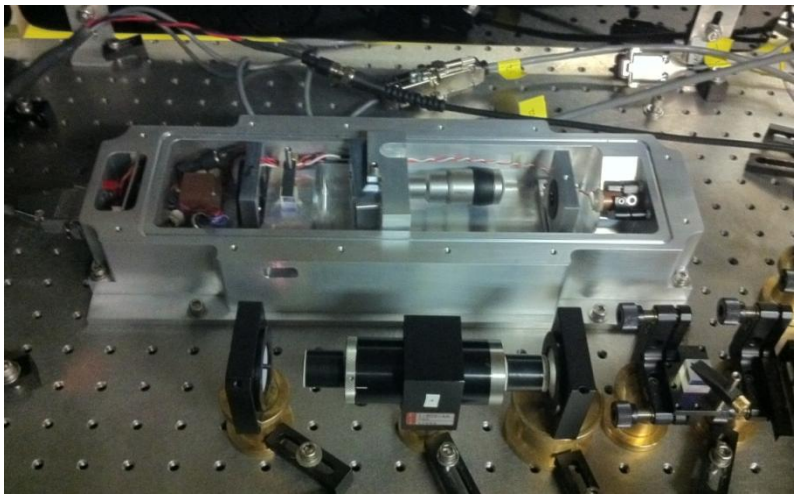

William Bowden
Damien Quentin
Jon-Paul Sun

Sponsored by
Dr. Kirk Madison
Quantum Degenerate Gas Lab
UBC Physics and Astronomy

Project Number 1174
ENPH 479
Engineering Physics Project Laboratory
University of British Columbia
January 23, 2012

Executive Summary

Atomic molecular and optical physicists require highly stable laser sources to cool molecules to ultracold temperatures. Last year, for our APSC 459 project we designed and characterized an interference filter-stabilized external-cavity diode laser (ECDL). This year's project was primarily focused on stabilizing this laser via a lock either to a second ECDL or to a $5S_{1/2}$- $5D_{5/2}$ two photon transition in rubidium. A variety of methods and experimental techniques were used to characterize the performance of a range of electrical and optical components, and to investigate key design parameters in order to achieve a stable lock.

In locking two ECDL's together, the two beams were coupled in order to generate a beatnote. The beatnote was then split and sent through a long or short fiber, then mixed and filtered such that an error signal generated from the phase difference was sent to the proportional and integral (PI) control system. This control system generated a slow and fast response, from which we could control and adjust the laser's frequency.

To lock to the $5S_{1/2}$- $5D_{5/2}$ two photon transition, we built an oven to house the cell and various optical components and heating elements, coupled to a photomultiplier tube. A beam was sent through the cell and oven, and reflected back such that the two beams were coupled within the cell to make the atoms fluoresce. A lock-in amplifier was used to generate an error signal from the detected florescence in order to control the laser's frequency.

For the two laser locking experiment we achieved a lock on the order of 300 kHz. There are a few more techniques that we can investigate to tighten this lock, including switching to photodetector with less noise and a self-heterodyne beatnote measurement with a 100 km optical fibre and a 1550 nm laser diode.

The rubidium locking technique was successful at achieving a lock on the order of 1.8 MHz. This lock can be reduced by addressing some of the broadening mechanisms responsible for widening the transition peaks of rubidium, as well as optimizing a few of our system parameters to produce an error signal with more gain.

Table of Contents

Table of Figures

1 Introduction

1.1 Background and Significance

1.1.1 Diode Lasers in Cold Molecule Physics

Ultracold molecules are molecules cooled down to the order of micro-Kelvins. Presently, there is a large focus on the creation of such processes as Bose-Einstein condensation, degenerate Fermi gases, and optical lattices. At these temperatures, dipole molecular gases are excellent systems to model physical phenomena such as solid-state systems, quantum phase transition (super-conductivity), and quantum information, among others.

Atomic cooling requires stable laser sources to match resonance frequencies and narrow spectral widths to maximize absorption efficiency. Atomic physicists are turning to diode lasers as a relatively cheap and effective alternative to conventional coherent light sources for their research. Being both small in size and not requiring elaborate cooling systems, diode lasers can be easily incorporated into most optical systems. However, the frequency instability of diode lasers requires complex locking mechanisms to fix the output frequency of the laser.

The desired application of this laser and frequency control system is to produce cold molecules from cooled atoms. In particular, we wish to form lithium-rubidium dimers, which exhibit many interesting quantum phenomena due to their internal structure and anisotropic interactions.

1.1.2 Making Cold Molecules

Below is a potential energy plot of the Li-Rb states. Ideally, we want the molecules to exist in the lowest, most stable energy state (marked by the bold red line). To achieve this state, a two-photon method is proposed (labeled with arrows *c* and *d*). First, the molecule is excited to an energy level in its first excited state (*c*). Next, the molecules experience stimulated emission and relax to the energy state (*d*).

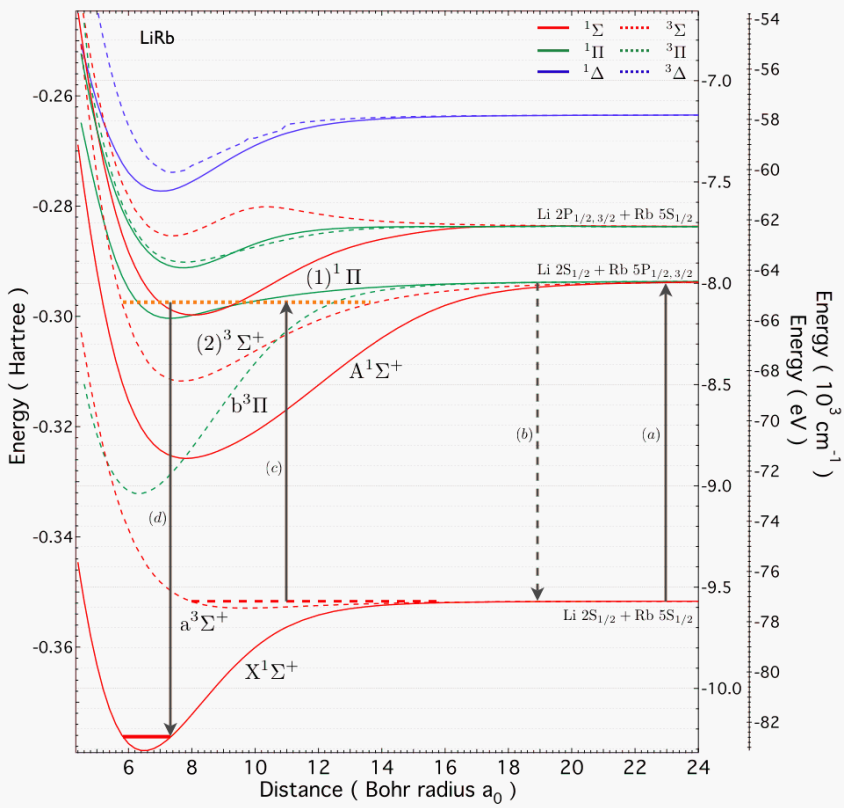

Figure 1 Potential energy plot of the different Li-Rb dimer states showing the laser-induced cooling transitions.

This process requires two laser sources: the first provides photons corresponding to the energy of the first transition and a second source is needed to put the molecule into its ground state. For this method to succeed, the frequency of both sources must be highly stable at precisely controlled set points.

This transition requires two stable laser sources with precisely controllable frequencies. One method to achieve this system is a frequency comb. A frequency comb is a series of sharp spikes in the frequency domain separated by a fixed, controllable, amount. If two signals are locked to the comb, the frequency difference between the two signals can be precisely controlled. The basic principal of operation is a single mode laser is dispersed into a multi-mode laser to form a comb of frequency elements.

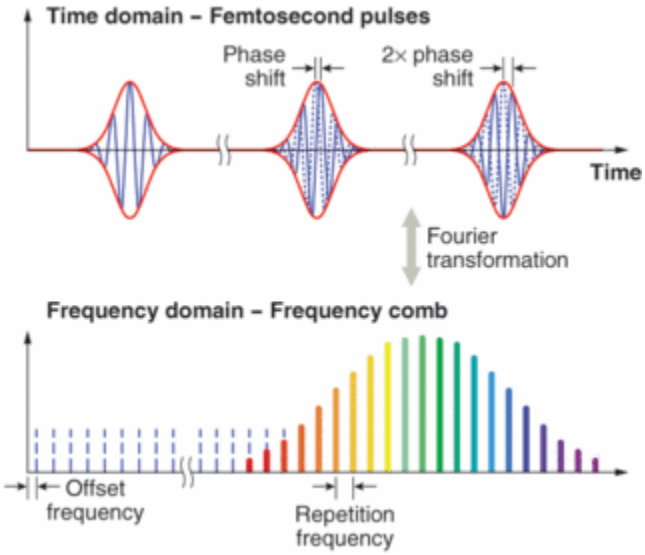

Figure 2 Temporal and frequency spectrums of a laser frequency comb. [5]

However, the stability of the comb is ultimately limited by the stability of the single mode input laser. Therefore, one of the main focuses of this project is to design a system capable of stabilizing a diode laser to be used as the input to the comb system.

1.2 Statement of the Project

The objective of this project was to design and construct a frequency lock for an interference filter-stabilized eternal-cavity diode laser (ECDL). This lock was achieved via two separate approaches: locking two ECDL's to each other, and locking a single ECDL to a $5S_{1/2}$ - $5D_{5/2}$ two photon transition in rubidium.

1.2.1 Two ECDL Lock

In this method, the beams from two ECDLs were superimposed to generate a beat note. The signal from this beat note was split and passed through short and long cables, which introduced a relative phase shift dependent on the frequency. The two signals were then mixed and filtered which produced a frequency dependent voltage signal due to the phase difference. This signal was used to stabilize the frequency of our laser using a control box capable of both proportional and integral (PI) feedback. This control box modulate the AOM, laser current driver, and piezoelectric transducer (PZT) controlling the laser's cavity length.

1.2.2 Frequency Lock to an Atomic Transition

Atomic references provide a stable reference necessary for laser locking. By stimulating a two-photon transition within a rubidium cell, we were able to successfully lock our laser to specific atomic transition. A small oven was designed and built to house the

rubidium cell, along with a lens and filter system to capture the fluorescence with a photomultiplier tube (PMT).

A lock-in amplifier was used to generate an error signal from the detected florescence. This signal was fed to a PI control system which was used to modulate the PZT and current driver.

1.3 Scope and Limitations

This report serves as a detailed description of the methods and experimental techniques used in the locking of an interference filter-stabilized external-cavity diode laser. These methods were used to characterize the performance of a variety of electrical and optical components, and to investigate key design parameters in order to achieve a stable lock. We present the results of the locking techniques and suggest experimental factors that can be modified to potentially improve the stability of the laser's frequency.

1.4 Organization

This report is divided into two sections, both of which outline a specific method used to stabilize the frequency of the lasers. These sections contain their own discussion, conclusion and recommendation based on the results this specific work.

Section two describes our work in locking two ECDL together to maintain a constant frequency differs by producing a beat note. This section also covers our analysis of the locking system characteristics and limitations.

Section three outlines our work in locking our laser's frequency to an atomic transition of rubidium. It will describe the basic theory of this technique, our experimental setup and finally out results.

Finally, we summarize our project deliverables, financial details of project and our future involvement in the project. We conclude with our recommendation based on the entirety of work on stabilize external cavity diode laser for potential applications in atomic cooling.

2 Two Laser Locking using Signal Mixing

2.1 Theory

Laser light at 780 nm oscillates at 385 THz, while fast photodetectors and spectrum analyzers are typically limited to bandwidths on the order of GHz. In order to measure the linewidth of two lasers at 780 nm, a beatnote must be produced. If the electric fields of the lasers can be represented by cosines

$$\boldsymbol{\varepsilon_1} = \boldsymbol{E_1} cos(\omega_1 t)$$
$$\boldsymbol{\varepsilon_2} = \boldsymbol{E_2} cos(\omega_2 t)$$

Where $\boldsymbol{E_1}$ and $\boldsymbol{E_2}$ represent the amplitudes of the fields and ω_1 and ω_2 are the frequencies of the lasers. Then the beatnote produced by multiplying the two fields corresponds to the sum and difference of the two frequencies

$$\boldsymbol{\varepsilon_1 \varepsilon_2} = \boldsymbol{E_1 E_2} cos(\omega_1 t)\cos(\omega_2 t) = \frac{\boldsymbol{E_1 E_2}}{2}\{cos[(\omega_1 - \omega_2)t] + \cos[(\omega_1 + \omega_2)t]\}$$

If the frequency difference of the two lasers is within the bandwidth of the photodetector, then the low frequency beat can be observed while the high frequency beat is filtered out.

If the two lasers are not stable and oscillate about some frequency, then the beatnote also oscillates. In order to measure the linewidth of the beatnote, it must first be locked to a stable center frequency. Two methods investigated in this report are the frequency mixer and the frequency/phase discriminator. The frequency mixer works much in the same as the beatnote is produced. After the beatnote is converted to an electrical signal by the photodetector, it is split and one branch is sent through a delay line and then recombined with the non-delayed branch in the mixer. The delayed signal will have a phase difference φ that results from travelling through a longer path to get to the mixer. If two signals seen by the mixer can be represented again by cosines where

$$\boldsymbol{\alpha_1} = \boldsymbol{A_1} cos(\omega t)$$
$$\boldsymbol{\alpha_2} = \boldsymbol{A_2} cos(\omega t + \varphi)$$

then the output of the mixer will again be the sum and difference of the arguments of the cosines

$$\boldsymbol{\alpha_1 \alpha_2} = \boldsymbol{A_1 A_2} cos(\omega t)\cos(\omega t + \varphi) = \frac{\boldsymbol{A_1 A_2}}{2}\{cos[\varphi] + \cos[2\omega t + \varphi]\}$$

If this signal is then passed through a low pass filter, only the *cos(φ)* term will remain. An important parameter in this method is the number of wavelengths *n* that fit into the delay line. Since the mixer sees the cumulative phase delay, small phase changes *Δφ* are effectively multiplied by *n* to produce a larger signal *cos(nΔφ)*. Therefore *n* acts as a scaling factor in the gain of the system. This DC signal can then be used as an error signal to lock the lasers.

An alternative approach to using a frequency mixer is to use a frequency/phase discriminator. This piece of equipment compares the frequency of the beatnote to a reference frequency, in this case produced by a direct digital synthesizer (DDS). When the frequencies of the reference and the beatnote are very different the discriminator produces an error signal that resembles a Heaviside function. This can be seen in Figure 3.

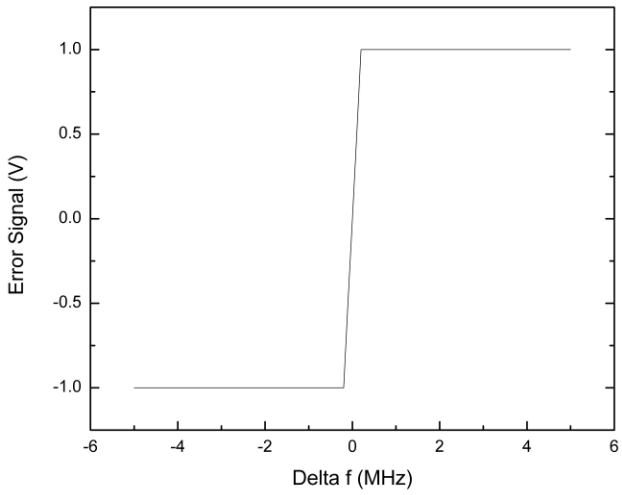

Figure 3 Error signal produced by frequency/phase discriminator for large frequency differences

At absolute frequency differences of less than 1 MHz, the discriminator switches to comparing the phase of the two signals to produce an error signal.

2.2 Methods

Two 780 nm interference filter-stabilized external-cavity diode lasers were used to produce a beatnote. One of the lasers was sent through a double-pass AOM before combining with the other laser.The resulting beatnote was sent to a receiver optical sub-assembly (ROSA) for photodetection. The ROSA converted the optical signal to an electrical signal before passing it to either a frequency mixer or a frequency/phase discriminator. The mixer and the frequency/phase discriminator each produced an error signal that was sent to a PI lock box which produced a slow output to modulate the piezoelectric transducer (PZT) driver and a fast output to modulate either the current driver or the AOM frequency.

Since most of the equipment used in this project did not have available documentation, a large range of characterization experiments had to be performed to fully understand the functions and limitations of all the components. The first unit in the chain is the ROSA, which produces harmonics when a certain power threshold is reached. This unit was characterized by measuring the power of the beatnote and its harmonics on a spectrum analyzer with varying laser powers.

The next unit in the chain is the frequency mixer. The intrinsic noise levels of the mixers were characterized by inputting a DDS tone and tuning the frequency until the error signal went to zero. At this point the noise was measured on an oscilloscope. Two different mixers were tested in this report, a level 7 and a level 23 mixer. The level of the mixer corresponds to the local oscillator (LO) power in dBm.

The PI lock box was characterized by measuring its frequency response to a sinusoidal error signal input. The PZT/mirror in the laser cavity also had its frequency response measured using the same method.

2.2.1 Experimental Equipment and Flow Diagram

The experimental setup for the two laser beatnote locking is shown in Figure 4 for the frequency mixer and Figure 5 for the frequency/phase discriminator.

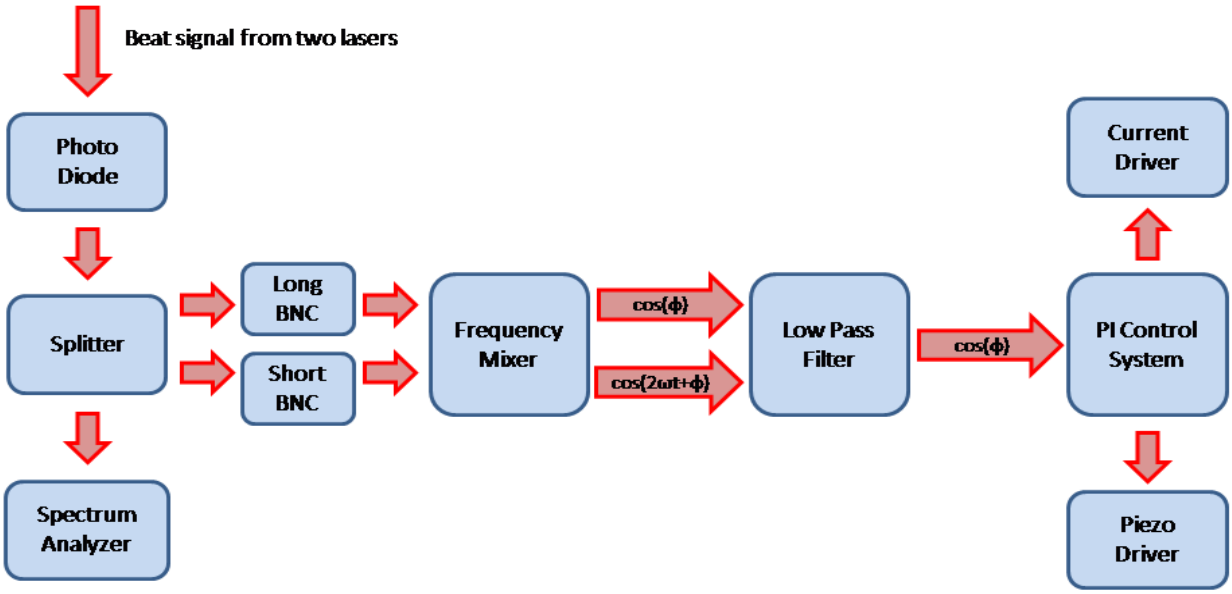

Figure 4 Beatnote error signal generation with frequency mixer.

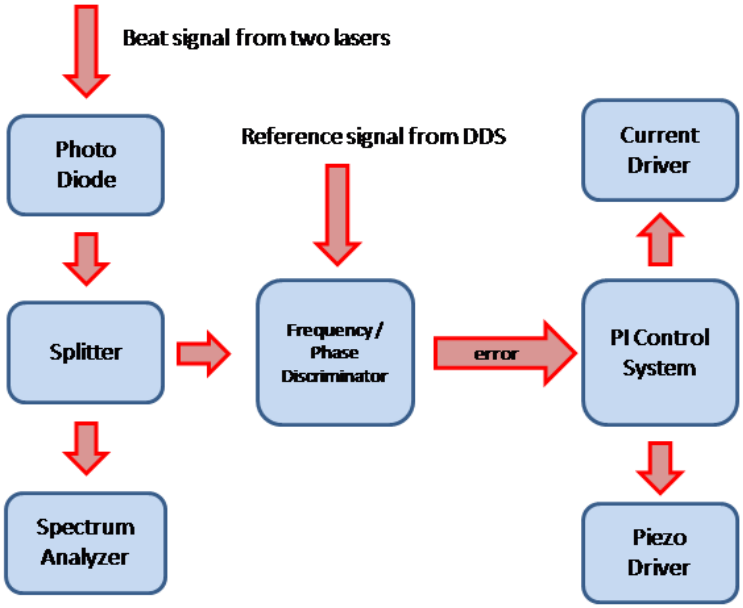

Figure 5 Beatnote error signal generation with frequency/phase discriminator.

2.3 Results and Discussion

The results of the power measurement of the third harmonic peak of the signal from the ROSA is shown in Figure 6. Below 300 µW total laser beatnote power, the third harmonic peak decays to the noise floor.

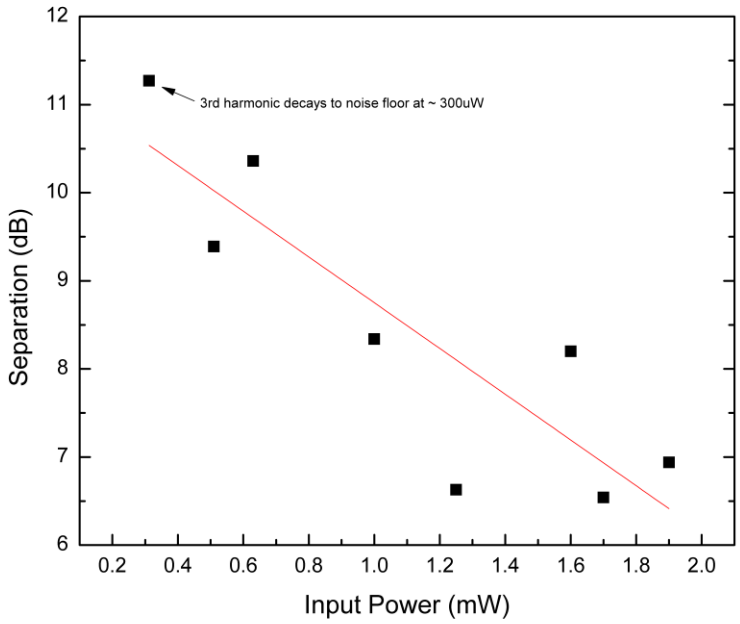

Figure 6 Separation between first and third harmonic peaks of output signal of ROSA as laser power is changed.

This gave us an upper bound on the input power to send to the ROSA to limit noise due to harmonics.

The amplitude and phase response of the lock box are shown in Figures 7 and 8. The slow response that is sent to the PZT driver rolls off after 100 Hz. The fast response then takes over and is responsive in the range 100 Hz – 10 kHz.

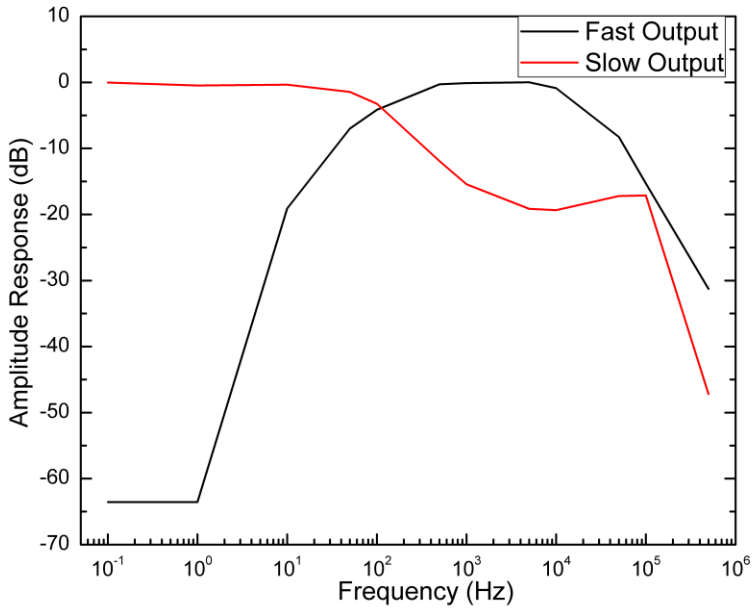

Figure 7 Fast and slow amplitude response of the lock box.

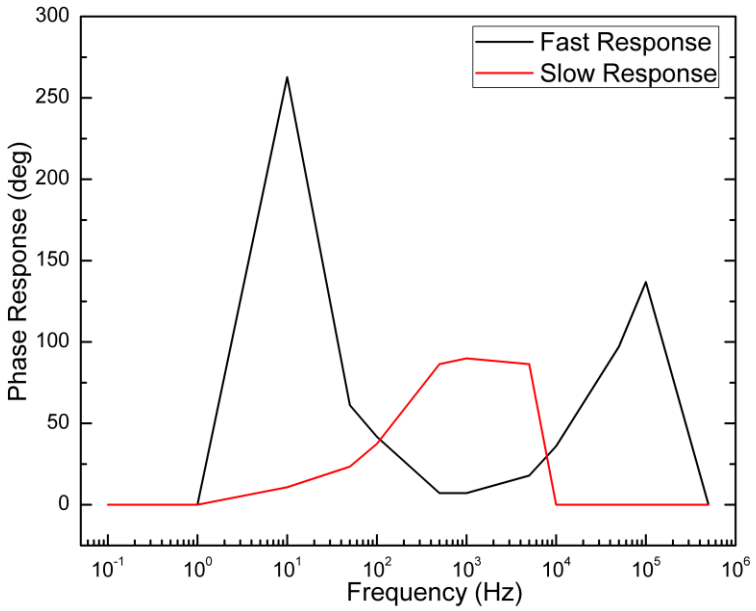

Figure 8 Fast and slow phase response of the lock box.

Since the slow response of the lock box drops off at 100 Hz, the PZT system was tested to determine its response. Figure 9 shows the frequency modulation of the PZT system

per volt output of the PZT driver. Due to the mass of the mirror mounted on the PZT, the system response drops off after 1 kHz.

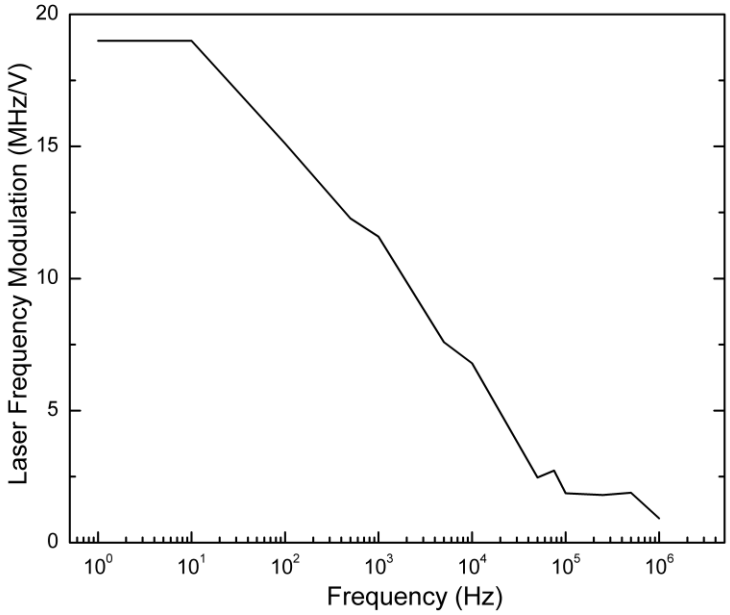

Figure 9 Laser frequency modulation response of the piezo.

The error signal of the level 7 mixer was mapped out over the range 73 to 77 MHz using a 45 m delay line with the DDS, as shown in Figure 10. Since we typically work with a beatnote at around 500 MHz with a 7.5 m delay line, 45 m was chosen to test with since it is dimensionally equivalent in terms of the number of wavelengths in the delay line. The signal level was measured in mV on an oscilloscope with 1 MΩ input impedance.

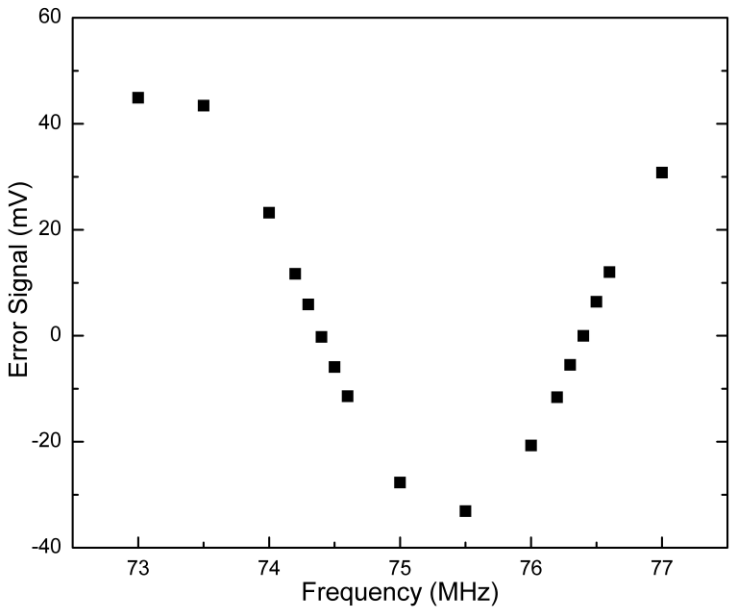

Figure 10 Error signal of the level 7 mixer with 7 dBm LO power, -19 dBm RF power, and 45 m delay line.

The output power of the mixer can be calculated from the radio frequency (RF) power minus conversion losses. Figure 11 shows the slope of the error signal about a zero crossing. The gain increases as the RF power increases since this results in the IF power increasing.

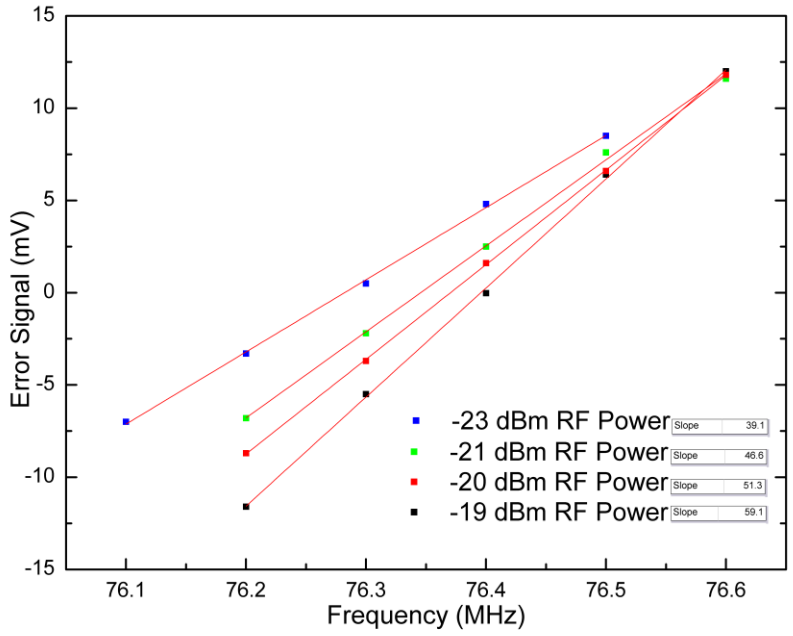

Figure 11 Error signal slope as the RF power is changed with a 45 m delay line.

Figure 12 below shows the error signal following the square root of the RF power by a scaling factor that is proportional to the conversion losses, the phase delay, and the input impedance of the oscilloscope.

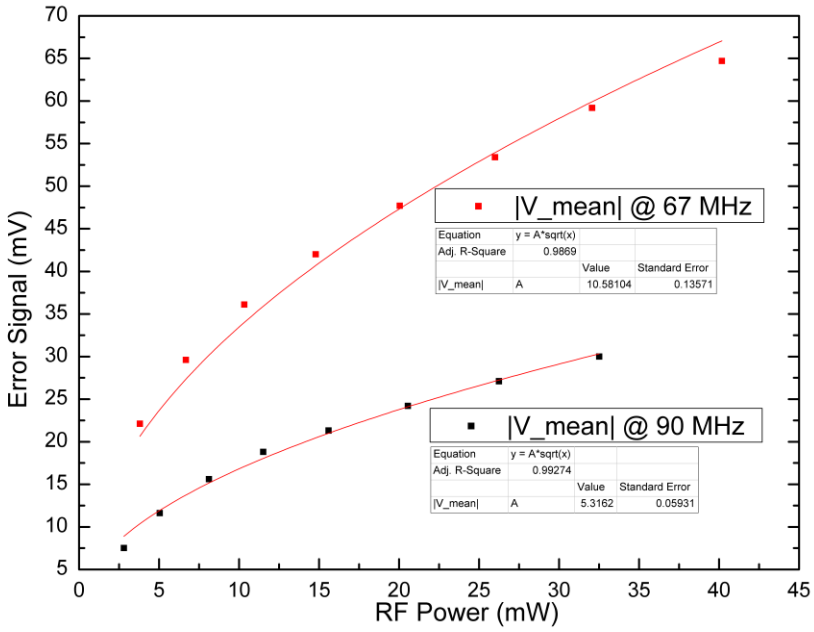

Figure 12 Error signal as a function of RF power.

The noise level in the mixer did not follow the square root of the power as expected. Shown in Figure 13 is the noise level versus RF power. The noise seems to plateau at higher RF power which should increase the signal to noise ratio (SNR). However, the absolute noise level in this mixer when operated at optimal power was still found to be too large to produce a tight lock. Attempts to lock the beatnote with this mixer resulted in a lock on the order of 300 kHz, which also happened to correspond to the noise when the error signal to frequency gain was calculated.

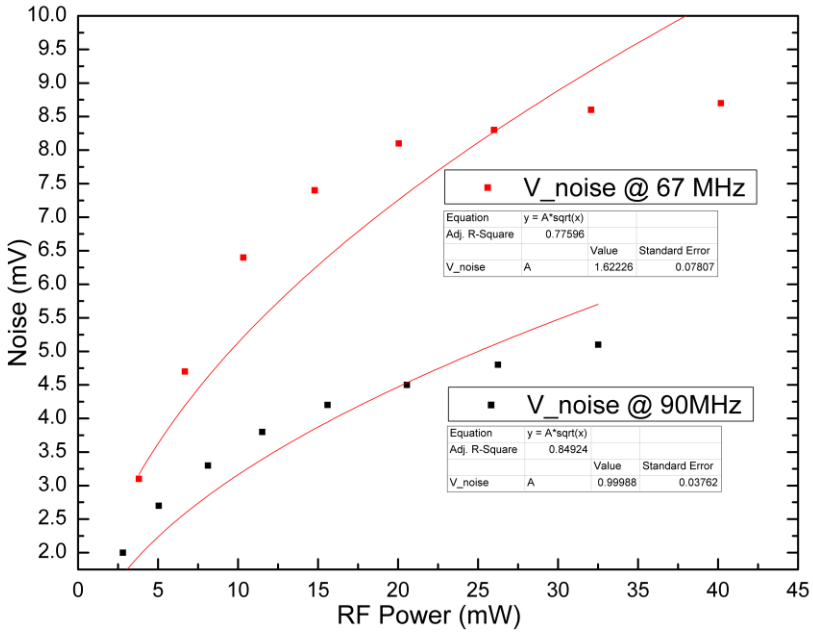

Figure 13 [description needed]

Another interesting feature of the frequency mixer method is the dependence on zero crossing frequency due to LO power. The mixer is basically a diode that gets turned on when the LO swings to a positive voltage. This allows transmission of the RF signal at the LO frequency, effectively sampling the RF signal. However, there is a minimum threshold power required to turn on the diode, so at lower powers the diode is on for a shorter time interval. What can be observed in Figure 11 is that the zero crossing shifts to higher frequencies for higher LO power. Figure 14 and 15 show the trend in zero crossing shifts as the LO power changes for both downward and upwards crossings, respectively. The slopes of these two plots indicate that the upward sloping zero crossings are approximately five times more sensitive to changes in power. This is important since the laser power randomly fluctuates, moving the zero crossing, and effectively increasing the width of the lock. A laser intensity fluctuation filtering circuit was designed to address this issue but has not been fabricated. Refer to Appendix 1 for details on this circuit.

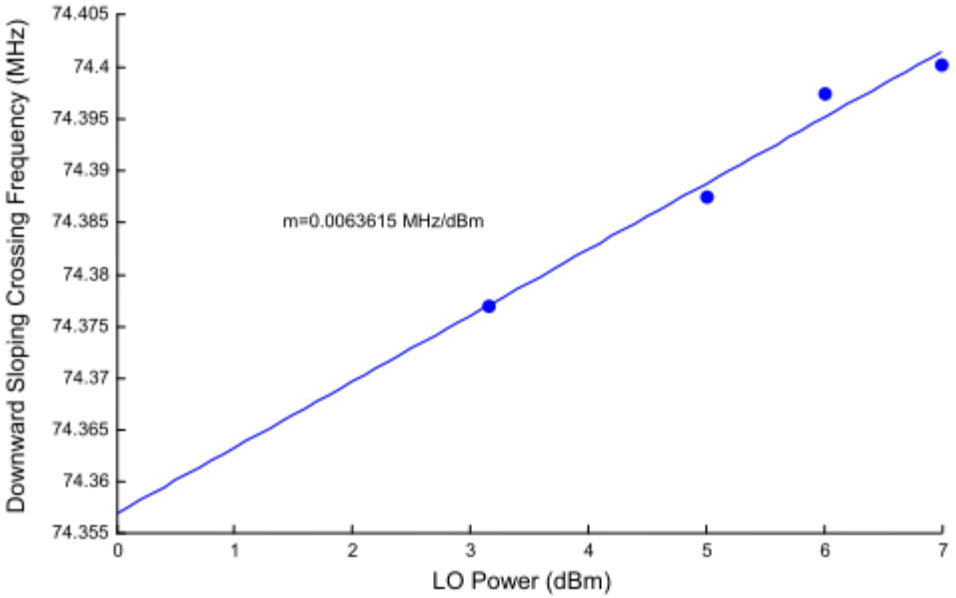

Figure 14 Downward sloping zero crossing dependence on LO power.

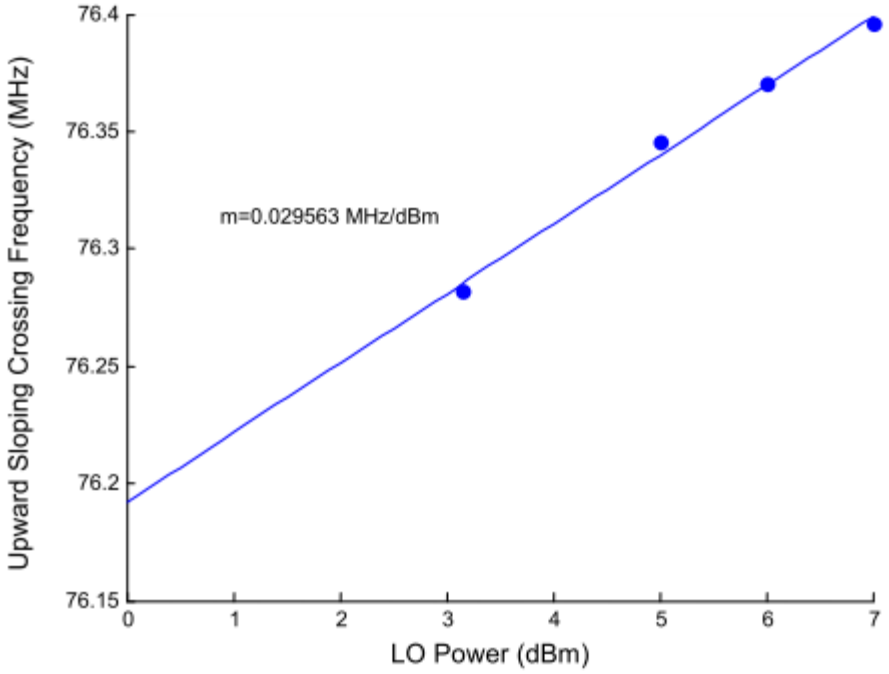

Figure 15 Upward sloping zero crossing dependence on LO power.

Figure 16 below shows the effect of changing the length of the delay line on the error signal gain. Since a longer cable can fit more wavelengths, the phase delay and the error signal scale with the change in number of wavelengths.

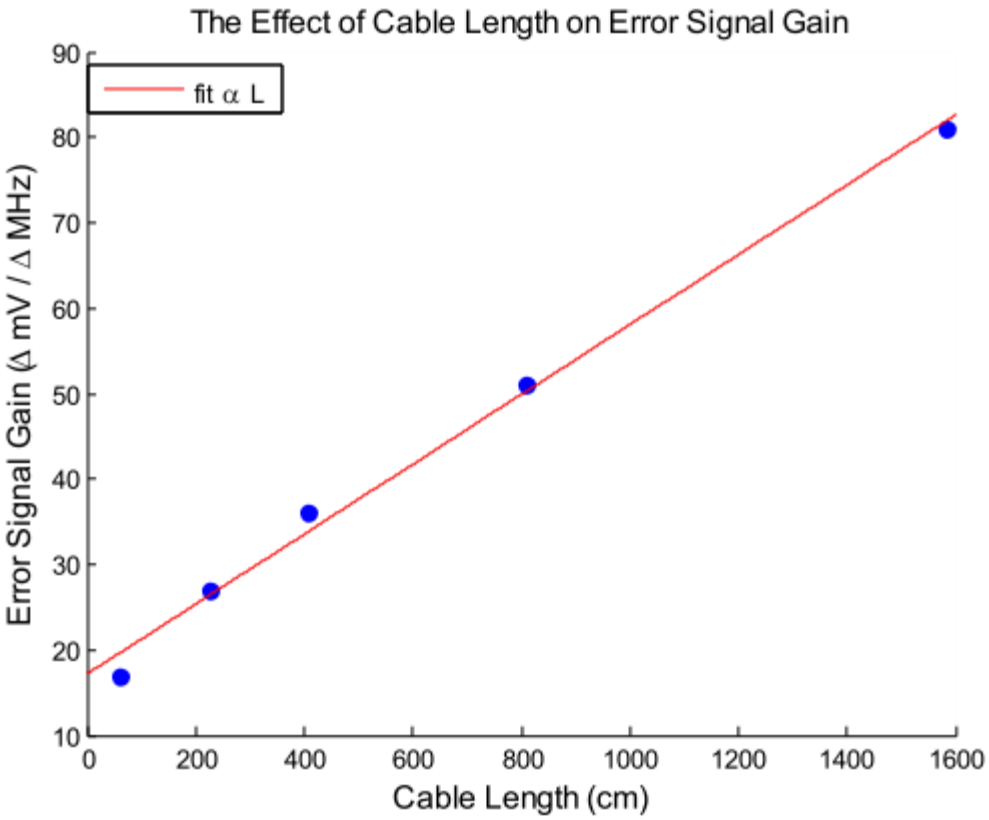

Figure 16 Error signal gain as a function of cable length.

However, a longer delay line also causes the zero crossings to be spaced closer together as shown in Figure 17. When the zero crossing separation is on the order of the frequency drifts of the laser, the error signal can move over a peak. This causes the PI control to force the laser to lock to the nearest zero crossing, resulting in a hop in frequency. Therefore, there exists an optimal delay line length that provides a large enough gain but is still stable in terms of frequency hopping.

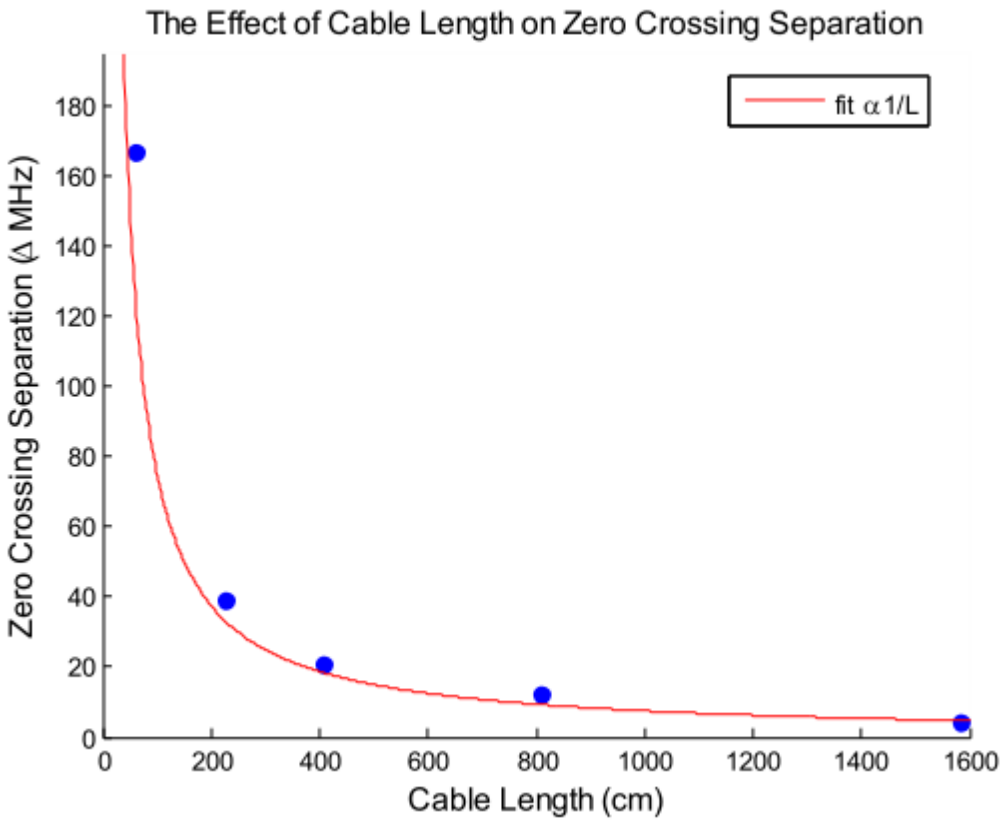

Figure 17 Zero crossing separation as a function of cable length.

Since the noise level on the low power mixer was found to be on the order of the lock, another mixer was used to increase the signal to noise ratio of the system. The new mixer takes a LO signal at 23 dBm. The output power of the mixer is dependent on the RF input power and the conversion loss of the mixer. The recommended RF power is typically ~10 dB below the LO. With 14 dBm RF power and 7 dB conversion loss, the intermediate frequency (IF) output power was 7 dBm. This resulted in a much larger signal as shown in Figure 18 The error signal output of the mixer depends on the phase difference of the two signals, which can be modeled as

$$e = A\cos\left(\frac{2\pi L}{c} f + \varphi\right)$$

where A is the amplitude of the signal, f is the frequency, L is the delay line length, c is the speed of the signal in the delay line, and φ is a phase correction. By fitting the error signal in Figure 18 to this model, we were able to calculate the velocity factor, which is the speed in the medium divided by the speed of light in a vacuum, to be 0.65 ± 0.01. This is close enough to the documented value of 0.66 for the RG58C/U coaxial cable used in this experiment. Confirmation of the model provides some intuition into the behavior of the zero crossing separation and error signal gain dependence on cable

length. The period of the sinusoid, or the zero crossing spacing is inversely related to the argument of the cosine

$$\Delta f = \frac{c}{L}$$

as observed in Figure 17. The derivative of the error signal with respect to frequency

$$\frac{\partial e}{\partial f} = -2\pi A \frac{L}{c} \sin\left(\frac{2\pi L}{c} f + \varphi\right)$$

is linearly proportional to cable length for a fixed frequency, as observed in Figure 16.

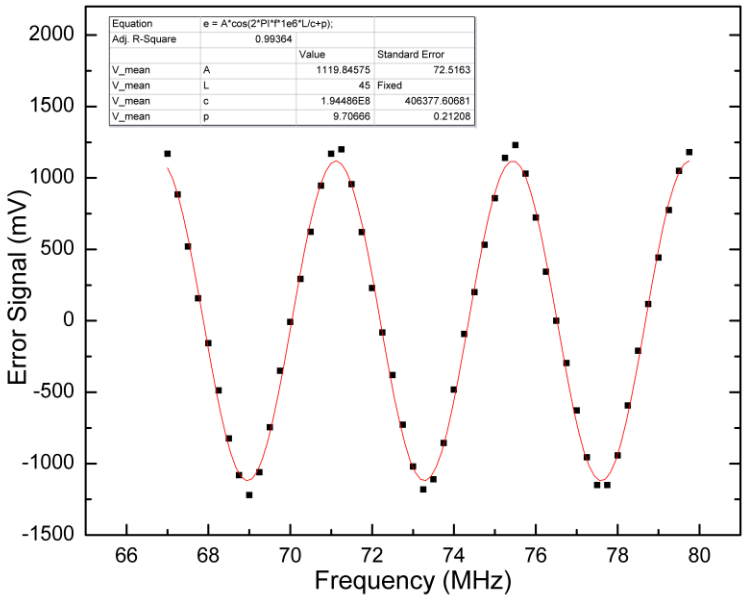

Figure 18 ZMY-2+ frequency mixer error signal with 23 dBm LO power, 14 dBm RF power and 45 m delay line.

The noise of this mixer was also able to go down to much lower levels than the previous mixer. However, when used to generate an error signal from the beatnote, the noise always corresponded to the 300 kHz linewidth of the beatnote when the frequency to error signal gain of the system was measured. This led us to suspect either the lasers are limited to a 300 kHz beatnote linewidth, or the ROSA is limiting the SNR.

The frequency/phase discriminator was then used to lock the beatnote. Since this method does not use the frequency mixer it can confirm that the linewidth we previously measured is not limited by the mixer. Figure 19 shows the result of this measurement. The FWHM was calculated to be 386 kHz by fitting a Gaussian to the data.

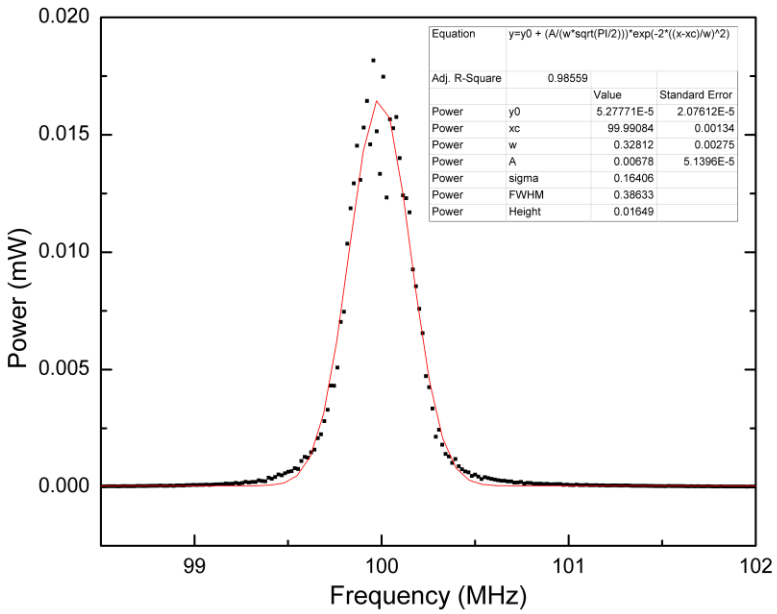

Figure 19 Frequency/phase discriminator lock showing a FWHM of 386 kHz.

2.4 Conclusion

In order to accurately determine the linewidth of the beatnote we need to determine the noise output of the ROSA to see if this is the limiting factor. To measure this we can tune the beatnote down to less than 100 MHz and use a slower photodetector to measure the linewidth.Since there is typically a tradeoff between noise and bandwidth, a slower photodetector should be able to produce a tighter lock if this is thelimiting factor. The beatnote can easily be tuned down to low frequencies by sweeping the PZT. The beatnote can be found using the high speed photodetector since it has a bandwidth of 1 GHz. It can then be swept down to below 100 MHz so that a slower photodetector can be used.An alternative method to producing a beatnote to measure the linewidth would be to lock two lasers independently to a Rb transition and beat the lasers together. Since the lasers would already be locked, the linewidth would depend on the tightness of the lock and the width of the two lasers. A third alternative would be to change the laser to 1550 nm wavelength and do a self-heterodyne beatnote measurement with a 100 km fibre. Figure 20 below shows the attenuation per kilometer in single mode fibre as a function of wavelength. Since the coherence length of our laser was found to be longer than the 10 km fibre we tested on for the previous report [1], we were unable to resolve a clean Lorentzian spectrum. We have a 100 km fibre available to test with, however the attenuation for 780 nm light is too much to detect a signal on

the other end. If we switched to a 1550 nm diode laser, we could do this experiment with the 100 km fibre.

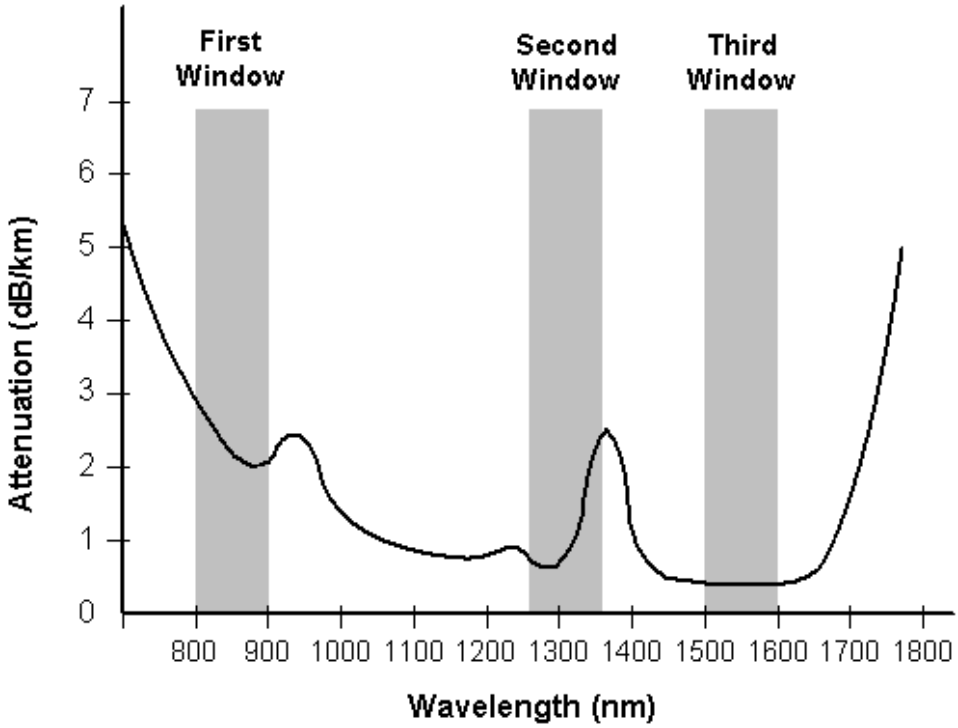

Figure 20 Attenuation in single mode optical fibre as a function of wavelength.

3 Laser Frequency Locking to an Atomic Transition of Rubidium

3.1 Atomic Transition Locking Theory

The discrete nature of the absorption spectrum of atoms provides scientists with a stable frequency reference to which they can compare other sources. Commercial vapour cells are available that contain purified atomic gases which can be used to stabilize the frequency of a diode laser. By tuning the frequency of a laser to match the energy of an atomic transition, the emitted fluorescence can be monitored and used in a feedback system to maintain a constant lasing frequency. For this specific application, we used a rubidium (Rb) gas reference cell and lock to the $5S_{1/2}$ - $5D_{5/2}$ two photon transition. The rationale for this choice will be outlined in the theory section.

3.1.1 Doppler Invariance.

Within the vapour cell, the Rb atoms have a distribution of velocities which leads to a Doppler shift of the energy of the incident beam. For a single photon transition, this velocity profile leads to a broadening of the absorption spectrum, i.e. atoms moving towards the beam could absorb photons with energy below the transition and atoms moving away from the beam could absorb photons with energy greater than that of the transition. If instead the beam was retro-reflected back onto the return beam such that the atoms in the cell experience two counter-propagating beams, this velocity dependence is negated.

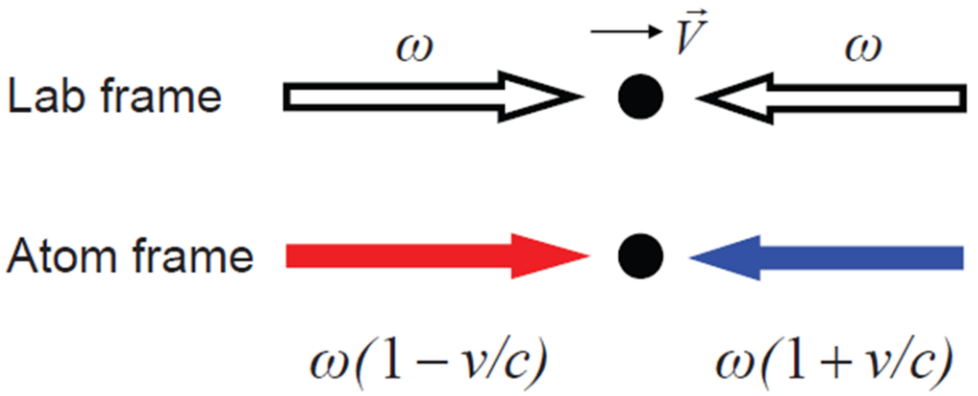

Figure 21. In the atom's frame of reference the incidents beams are Doppler shifted due to the atoms velocity [4]

To illustrate this point, take an atom with velocity *V* moving towards one of the beams (see Figure 21). The atom then simultaneously absorbs two photons both with frequency ω in the lab's frame of reference. The effect of the velocity in the atom's frame of reference will Doppler shift the frequency by a factor of (1+v/c) for the beam

propagating opposite to the atom's path and (1-v/c) for the beam moving parallel to the velocity. Hence, the total energy of this transition is

$$E = \hbar\omega\left(\left(1+\frac{v}{c}\right)+\left(1-\frac{v}{c}\right)\right) = 2\hbar\omega$$

Therefore the transition is invariant to the atom's velocity and non-Doppler broadened. However, the energy of the photon must now be half that of the transition energy. The complete absorption and emission process is shown below in Figure 22. A ground state Rb atom ($5S_{1/2}$) is excited to the $5D_{5/2}$ state where it then relaxes to the $6P_{3/2}$. From this state, it returns to the ground state by emitting a photon at 420 nm. The 420 nm fluorescence is detected by our system. The two photon transition ensures the excitation source and emitted signal are at different wavelengths allowing the scattered laser light to be filtered out without attenuating the emission signal.

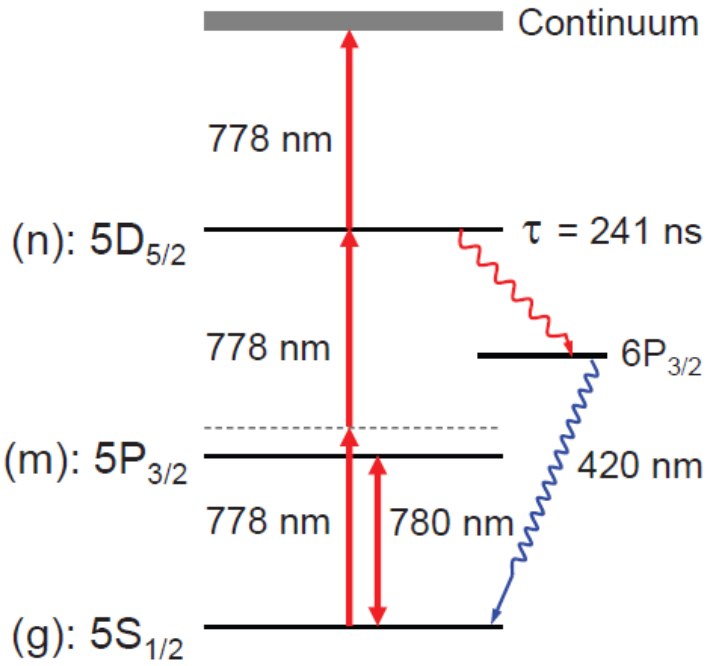

Figure 22 Schematic of the absorption and emission of the $5S_{1/2}$ to $5D_{5/2}$ two photon transition. [4]

3.1.2 Selection Rules

The ground state of the lone valence Rb atom is the $5S_{1/2}$ state, where the *5* denotes the principal quantum number, *S* is the orbital number and ½ denotes the sum of the orbital momentum and spin. The total angular momentum, *F*, for the state is the sum of the electron spin, the nuclear spin and orbital angular momentum. The nuclear spin, *I*, differs for the different Rb isotopes. For example, the nuclear spin for ^{87}Rb is equal to 3/2 and for ^{85}RB, *I* is equal to 5/2. The total angular momentum couples to the magnetic

field produced by the spin of the nucleus and leads to an energy splitting of the transition peaks. This phenomenon is known as the hyperfine splitting and the exact structure of the resulting spectrum can be calculated by the two photon transition operator given by [2]

$$\frac{(2F_g+1)(2F_e+1)\begin{pmatrix} J & 2 & \frac{1}{2} \\ F_g & I & F_e \end{pmatrix}^2}{2I+1}$$

where F_g and F_e are the total angular momentum of the ground and excited states, respectively, ½ is the electron spin and the factor of 2 corresponds the value of the momentum of the two absorbed photons. An example of a possible hyperfine transition would be ^{85}Rb in the $5S_{1/2}$ ground state with F_g equal to 3 (the sum of *J+I+S*) going to the $5D_{5/2}$ state where F_e can differ from F_g by any integer value from -2 to 2 due to two photons' momentum. This leads to five distinct energy peaks, the last of which is very weak. This transition spectrum is shown below:

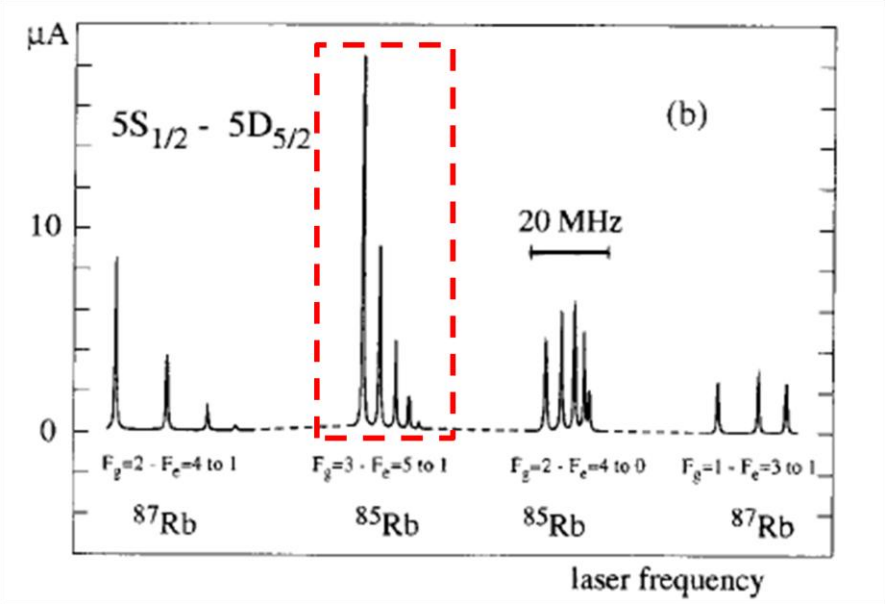

Figure 23 Emission spectrum of Rb for two isotopes (^{85}Rb and ^{87}Rb) highlighting one of the hyperfine transition families outline above. [2]

3.1.3 Broadening mechanisms

3.1.3.1 Transit Time Broadening

The atoms in the gas cell interact with the beam for a finite time. This time constant (τ) is determined by the velocity (v_{Rb}) of the atoms and beam width (W) by the following formula

$$\tau = \frac{W}{v_{Rb}}$$

The velocity of the gas is related to its kinetic energy, which is normally distributed due to Boltzmann statistics with mean energy k_BT, where T is the temperature of the cell. Therefore, the mean time the atoms spend interacting with the beam is

$$\tau = \frac{W}{\sqrt{\frac{2k_bT}{m_{Rb}}}}$$

where m_{Rb} is the mass of the rubidium atoms. This time constant broadens the energy due to the Heisenberg uncertainty principle. Using the uncertainty principle, we can determine the frequency broadening

$$\Delta E = h\Delta f = \frac{\hbar}{2\tau}$$

From the above expression, we find that

$$\Delta f = \frac{1}{4\pi W}\sqrt{\frac{2k_bT}{m_{Rb}}}$$

3.1.3.2 Magnetic Field Broadening

In the presence of an external magnetic field, the hyperfine structure can be distorted due to the induced magnetic potential energy. This is known as the Zeeman effect and the resulting energy (U) due to the external field is given by

$$U = -\vec{\mu} \cdot \vec{B}$$

where $\vec{B}$ is the magnetic field and $\vec{\mu}$ is the magnetic moment. The magnetic moment is defined as

$$\vec{\mu} = \frac{\mu_B g\vec{J}}{\hbar}$$

where $\mu_B$is Bohr magneton, g is the g-factor and $\vec{J}$ is the total angular momentum. Therefore, it is important that we have small, relatively static magnetic fields within the

oven to maintain a constant emission spectrum. This is critical to ensure high-sensitivity frequency locking.

3.1.4 Pump Probe Alignment tests using Saturated Absorption of a Single Photon Transition

The velocity distribution of atoms within a gas was accurately determined by Maxwell to be normally distributed according to Boltzmann statistics. This range of velocities broadens the absorption spectrum of a gas since the energy of irradiated photons is Doppler shifted. By having two counter propagating beams it is possible to saturate a range of atoms with a specific velocity. Taking advantage of this effect, we can align the incident and retro-reflected beams. The experimental setup can be seen in Figure 24.

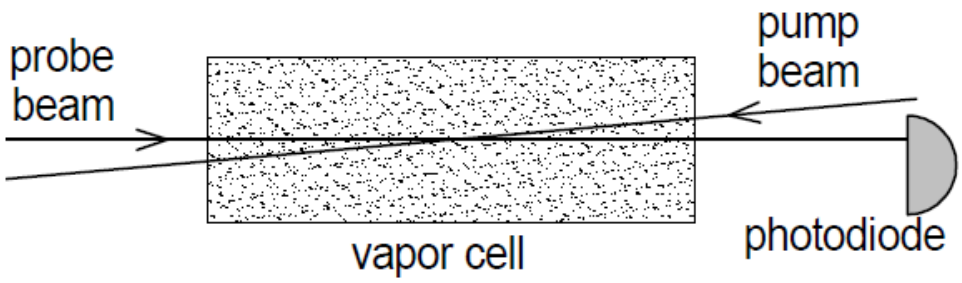

Figure 24 Experimental set up for the saturated absorption measurement.

By convention, the incident beam is known as the *probe beam* while the return beam is the *pump beam*. Due to Doppler shifts, the probe beam sees a transitional absorption frequency, v_{probe}'',

$$v''_{probe} = v_0\left(1 - \frac{v}{c}\right)$$

where v_0 is the absorption frequency in the lab reference frame, v is the atom's velocity component along the beam path and c is the speed of light. The pump beam has an absorption frequency given by

$$v''_{pump} = v_0\left(1 + \frac{v}{c}\right)$$

This Doppler shift in absorption will have the following effect on the distribution of atoms in the ground state at a given velocity.

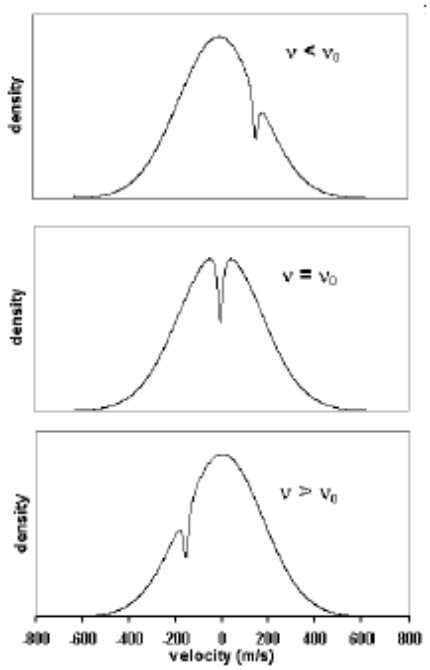

Figure 25 Absorbed photon with matching Doppler corrected energy excites electrons to higher energy levels.

These spectral dips of a two level atom model are formed by either the pump or probe beam depending on the frequency in a process known as hole burning. When v=0 and both beams are in resonance with the stationary atoms, the transition is said to be saturated. The probability distribution between energy levels is given by

$$P_0 - P_1 = \frac{1}{1+2\frac{I}{I_{sat}}}$$

where I is the laser intensity and I_{sat} is the intensity when stimulated emission is equal to spontaneous emission. By increasing the intensity at the resonance frequency, the gas becomes less absorbent which leads to signal dips in the photo diode voltage signal. These signal dips require the beams overlap and therefore we can use this method to verify our optical alignment.

3.2 Atomic Transition Locking Methods

3.2.1 Experimental Setup

Below is the optical setup of our experimental system used to lock the laser to the two photon transition.

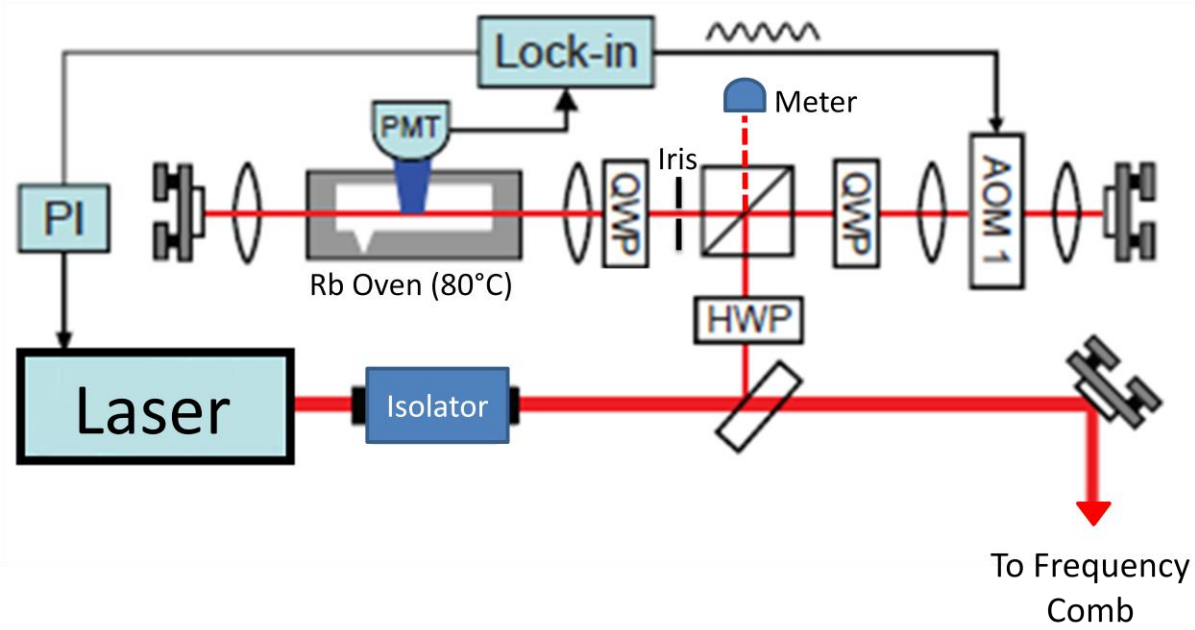

Figure 26 Experimental setup for the two photon transition showing the optical components and electronic detection system. [4]

The beam passes through an optical isolator to prevent back reflection into the laser which can destabilize the system. The laser is an interference stabilized external cavity diode laser and a more detailed description of its specifications can be found in [1]. The beam enters a polarization-dependent beam splitter. The half-wave plate (HWP) is used to ensure the incoming beam is entirely reflected to the right. The beam then travels through an acousto-optic modulator. The output beam has an angular displacement which depends on the acoustic frequency given by

$$\sin\theta = \frac{m\lambda}{2\Lambda}$$

where θ is the defraction angle, m is the deflection mode, λ is the beam wavelength and Λ is the wavelength of the acoustic waves. The deflection of the beam should be minimized as it affects the alignment of the system. By passing through the AOM twice and taking opposite modes for the forward and reverse beams (m=±1), the angle of the beam will remain constant with frequency modulation.

In the double pass AOM set up, the beam goes through a quarter wavelength plate (QWP) twice so it will be entirely transmitted through the cube on its return pass to the cell. An oven was designed to house the rubidium cell. The oven heats the cell to 80 ^{o}C and prevents unwanted light from entering the detection system. The cell is heated to increase the density of the gas which enhances absorption. The oven contains a collection of optics to capture the fluorescence and focuses it onto the photomultiplier tube. The optics contain coloured glass to filter out the 778 nm light and pass the 480

nm light. The beam passes though another QWP because absorption of circularly polarized light is higher than that of linearly polarized light. The beam entering the oven is approximately 10 mW in power and is focused to a beam waist of approximately 70 µm using a convex planar lens (focus = 120 mm). The beam is retro-reflected using a lens (focus = 60 mm) and a planar mirror which form a cat-eye configuration. The planar mirror is placed on a micrometer stage to set the distance from the lens. This is done to ensure the size of the incoming and return beams are matched and overlap. Unmatched beam modes can lead to a broadening of the signal. The reflected beam passes through an iris and is reflected off the beam splitter cube and into a power meter (the dotted line in Figure 26). By adjusting the mirror to maximize the return beam through the iris, we can ensure the two beams are overlapped over the entire beam path.

Next, the laser is tuned to the single photon transition of Rb ($5S_{1/2}$-$5P_{3/2}$) and the absorption spectrum is detected by sweeping over the frequency range by modulating the length of the cavity using the PZT. The saturated absorption dips are observed to ensure the beams are spatially overlapped. Fine adjustment of the mirror angle and position are made to maximize the dip depth.

3.2.2 Signal Detect (Photomultiplier tube and Lock-in Amplifier)

The two photon signal is very weak as the probability of simultaneous absorption is low. The approximate power of the signal is 4 pW [3]. Therefore, to detect the signal a photo-multiplier tube and lock-in amplifier were needed. The lock-in amplifier is used to isolate our signal from the background noise of the PMT's output to produce an error signal. The laser frequency is modulated to provide the lock-in amplifier with a reference at a frequency ω. A triangle wave then ramps the PZT at a rate of 0.1 Hz to vary the laser's external cavity length, thus changing the frequency. In doing so, the laser sweeps over the entire absorption spectrum while the optical frequency is modulated at ω via the AOM. The lock-in amplifier then demodulates the output florescence signal with a sine wave at a frequency ω. The matching frequency in the signal will mix to a constant DC value, while all other contributions to the signal will be at various frequencies. By integrating the input signal for a specific time constant (τ), the constant value will scale proportionally while all other frequencies will oscillate about zero. In that way, only the specific frequency of interest is amplified. The frequency range scanned over by the PZT during the integration time (τ) defines the spectral resolution of the system. The shorter τ is, the better the resolution, but this comes at the cost of decreasing the signal-to-noise ratio.

As the laser's frequency approaches the Rb cell absorption frequency, the amplitude of the fluorescence signal increases. As shown in Figure 27, whether the output florescence is in phase or perfectly out of phase with the modulation signal depends on which side of the peak the frequency is set.

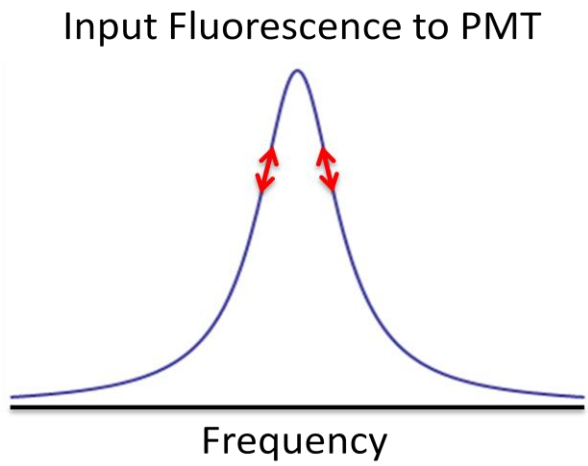

Figure 27 Florescence peak as a function of frequency. The red arrows represent the frequency modulation of our laser source.

However, if the frequency is already at or near the peak where the derivative is zero, frequency modulation will lead to no fluctuations in intensity. Therefore, the lock-in amplifier will detect no signal when the laser is at resonance. Hence, the lock-in amplifier differentiates the input signal (Figure 28). The zero crossing of the error signal corresponds to the florescence peak.

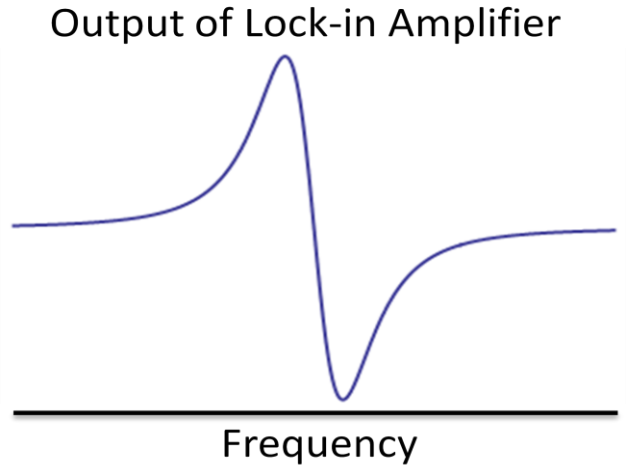

Figure 28 Output signal of the lock-in amplifier after the signal from Figure 24 is demodulated.

This error signal is then sent to a PI control module to provide fast and slow error control to the current driver and piezoelectric transducer.

3.2.3 Experimental Equipment

For our experimental setup we needed a laser capable of outputting 778nm light, a lock-in amplifier, a rubidium gas vapour cell, an oven to house the Rb cell, a photomultiplier tube and a feedback control box. The lock-in amplifier is a Stanford Research Systems

SR830 DSP. The Rb cell was purchased from Thorlabs and contains Rb gas which has an isotope concentration equal to that of its natural abundance. Details concerning the oven can be found in §3.2.3.1. We tested two PMTs, one manufactured by EMI (model 9558 B) and the other by Burle (model number C31034A), but ultimately decided to use the latter. The rationale for this decision is outlined in §3.2.3.2. Finally, the feedback control box was manufactured by the UBC Physics Department electrical shop and provides basic proportional and integral feedback with variable gain.

3.2.3.1 Rubidium Cell Oven

The oven was fabricated out of polycarbonate (which has an upper working temperature of 115-130 ^{o}C) and aluminum. The vapour cell is housed in a copper pipe which is electrically insulated with Kapton tape and wrapped with NiCr heating wires. The tube is heated using the NiCr wires and a Variac transformer operating at 10 V peak-to-peak and 60 Hz. We chose to heat the copper tube directly using the wire, rather than heating the entire oven because of concerns of warming the PMT. When heated, the PMT's cathode produces thermal electrons which leads to increased noise. The inside of the tube is lined with Mylar sheets to increase the amount of collected florescence by a factor of two by doubling the collection angle (see Figure 29). Next to the cell is a lens (f = 25.2 mm) to collect the light. The lens focuses the point source to a collimated beam. The collimated beam is then focused using a second lens (f = 100 mm) onto the PMT. The oven is capable of holding two different PMT models.

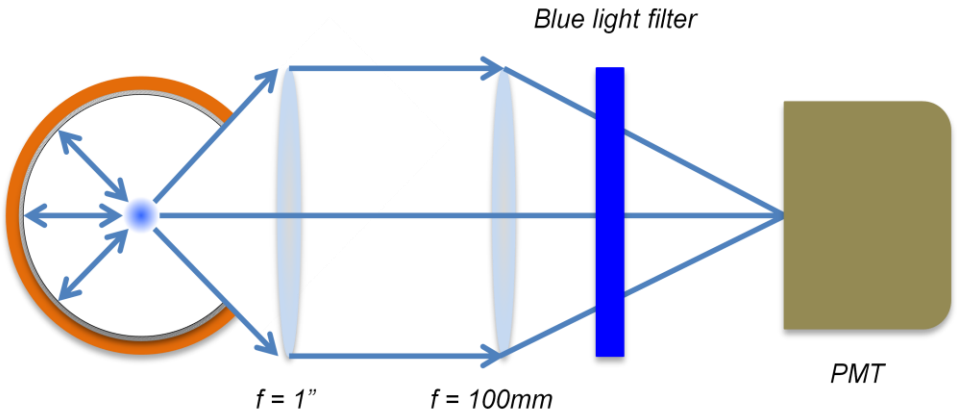

Figure 29 Optics used to capture the fluorescence. By lining the tube with Mylar we can collect the light reflected by the walls.

The width over which fluorescence can be collected is 2.54 cm. The length at which fluorescence is possible can be approximated to be the Rayleigh length, Z_R, of the beam

$$Z_R = \pi \frac{w_0^2}{\lambda}$$

where w_0 is the beam waist. For our beam parameters, the Rayleigh length is 1.95 cm. Below are two figures showing the constructed oven and inset with a Solidworks model. The first shows the entire assembly while the second shows the internal cavity and heating enclosure. The Rb cell is housed inside the Kapton/NiCr wrapped copper tube. There are two layers of heating wire wrapped in opposite directions separated by Kapton tape. This was done to cancel the magnetic fields induced by the wires.

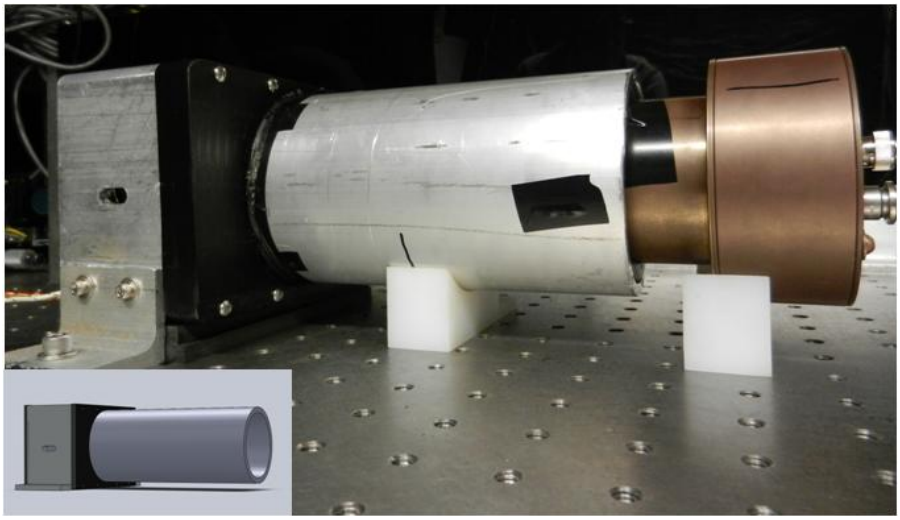

Figure 30 The oven is secured to the table and the PMT is fit into the holding tube using a rubber retaining ring. The oven was modeled in solid works.

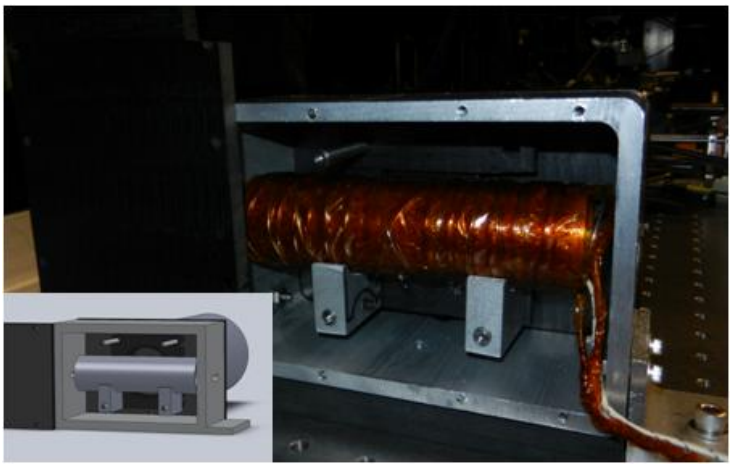

Figure 31 The heating tube used to house the gas cell. The tube is thermally isolated from the external housing to limit heat loss.

3.2.3.2 Photomultiplier Tubes

We had access to two PMTs. We decided to use the one manufactured by Burle as its cathode material was less sensitive to red light and would filter out the background

scattering of the laser. The frequency response of the PMT is important as it limits the maximum frequency at which the lock-in amplifier can modulate the signal. Typically, the 1/f noise (pink noise) of the system dominates the noise spectrum at low frequencies. Therefore, the modulation of the lock-in amplifier reference should be at higher frequencies so that the 1/f noise does not corrupt the signal. The frequency response of the detection system is defined by the input impedance of the lock-in amplifier and the capacitance of the PMT. The input impedance of the lock-in amplifier is 10 MΩ. The capacitance of the PMT is not specified on the datasheets. We tested the frequency response of the system and the results can be found in §3.3.1.

3.3 Results

3.3.1 Frequency Response of the PMT

We investigated the capacitance of both PMTs by modulating the laser's intensity over a range of frequencies and detecting the power fluctuations. The frequency response of both PMTs is shown below.

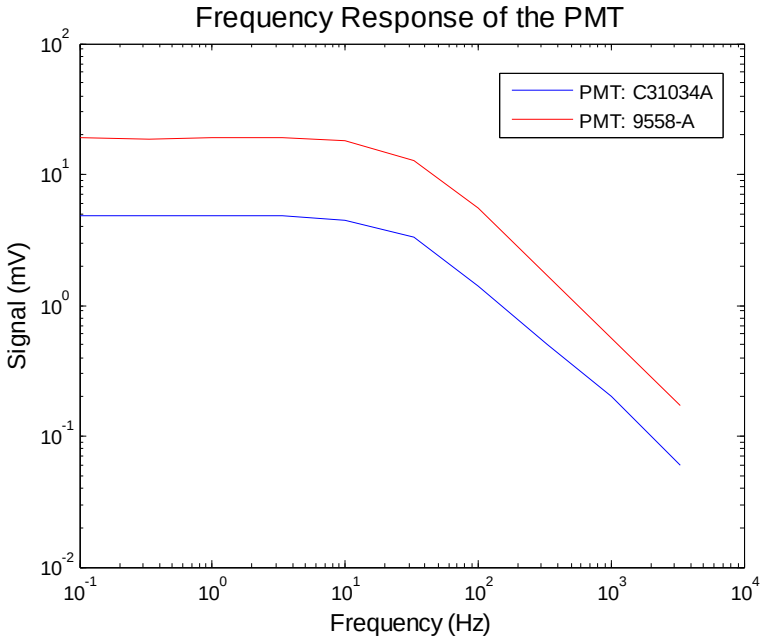

Figure 32 Frequency response of the PMTs and lock-in amplifier system.

The output capacitances of both PMTs is very high which leads to both devices having -3 dB frequencies of approximately 10 Hz. This prevents us from modulating at high frequencies to eliminate noise.

3.3.2 Example of Pump Probe Absorption test

To ensure the beams are collinear and overlap, the laser was tuned to the single photon transition at 780 nm. The following figure shows the saturation dips caused by the

return beam of the $5S_{1/2}$-$5P_{3/2}$ transition. If the dips are not present, the two photon transition is not possible. The dip depth is maximized by adjusting the mirror angle to increase the overlap of the beams. The mirror position with respect to the focus of the second lens is also adjusted to change the return beam's width.

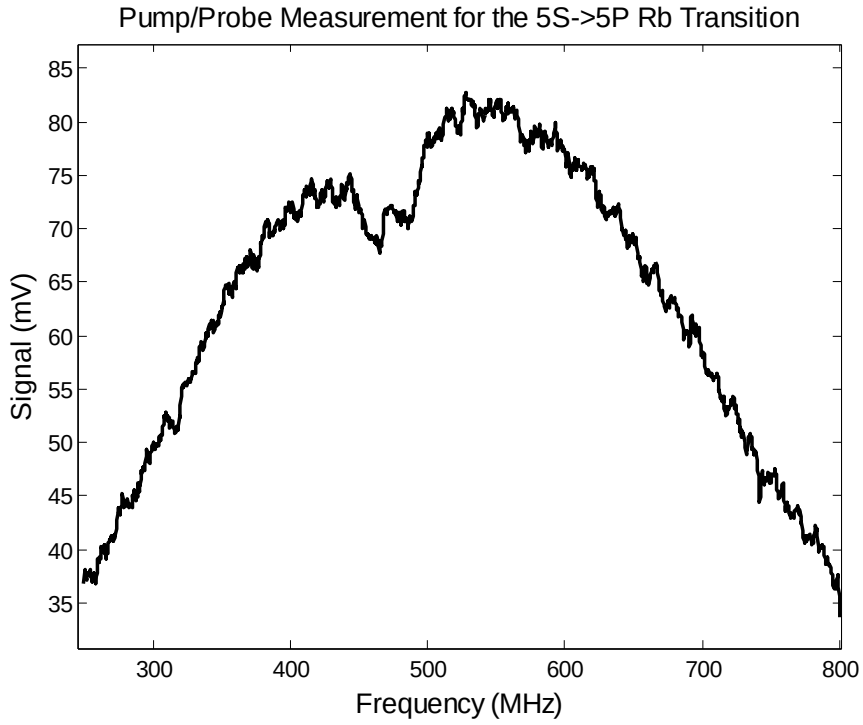

Figure 33 Florescence spectrum showing the saturated absorption dips of the single photon transition (5S to 5P)

3.3.3 Florescence spectrum

To ensure that we are in fact exciting the correct $5S_{1/2}$ - $5D_{5/2}$ transition, we compared our emission spectra to published results. We can only confirm the features are in approximately the correct spectral location because we cannot measure the exact frequencies as the resolution limit of wavelength meter is 75 MHz. We can however compare qualitative similarities such as the number of peaks, relative peak height and peak width. Below are two plots comparing the ground state of ^{85}Rb with angular momentum (F_g) equal to 2 and 3 with work published by Dr. Nez in the Journal of Optical Communications.

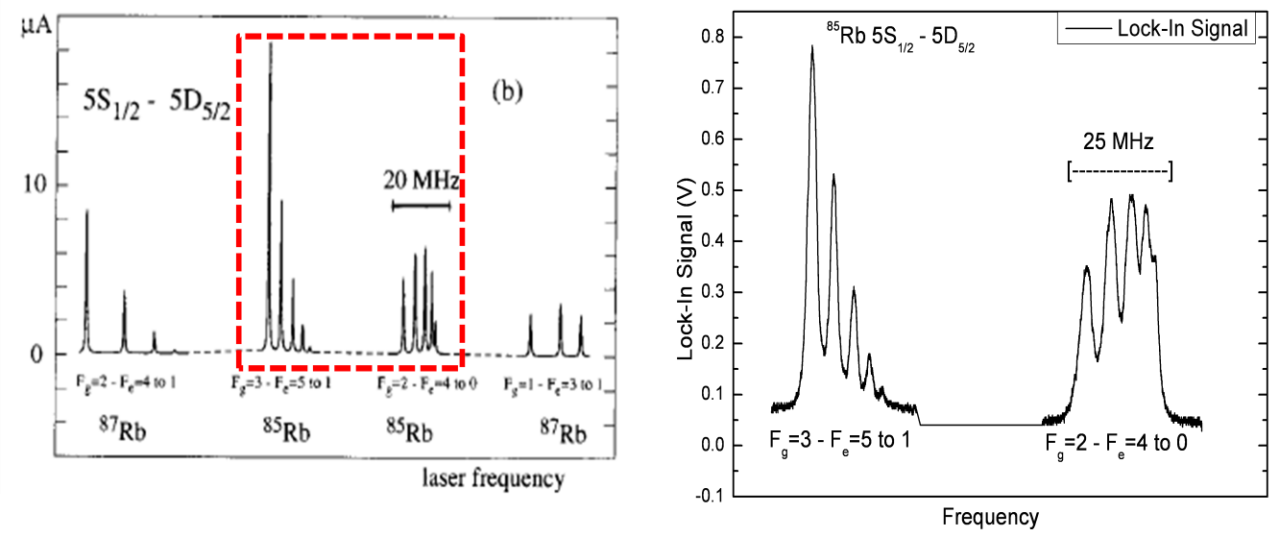

Figure34 Comparison of published spectra for the hyperfine structure of the 5S to 5D transition to our experimental results. [2]

Both hyperfine spectra agree in the number of peaks and relative peak heights. The natural linewidth of these features is 300 kHz [2]. A plot of the $F_g=3$ to $F_e=5$ florescence transition peak is shown in the following figure. A Lorentzian model was fit to the peak, which yielded a linewidth of 1.68 MHz.

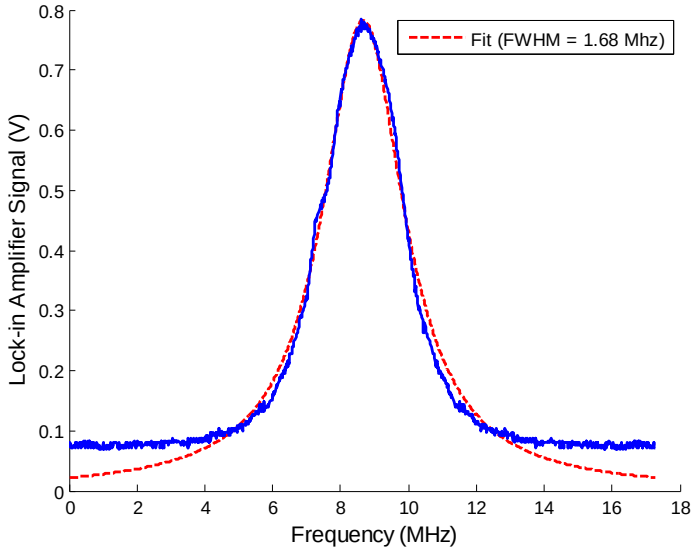

Figure 35 The $F_g=3$ to $F_e=5$ florescence peak of the 5S to 5D transition fit to a Lorentzian model. The fit gave a linewidth of 1.68 MHz.

The background light defined a noise level which prevented us from resolving the wings of the peak. The peak was significantly broader than its natural width. The linewidth of the feature is defined by three factors: a) the natural feature linewidth, b) the laser's linewidth and c) system dependent factors. Given that the laser's linewidth is on the order of 10 kHz [1], the broadening is primarily due to these external factors. These factors include misalignment of the beams, power broadening, transit time broadening and external magnetic fields. Given the beam parameters and the heat of the cell, the transit time broadening is approximately 300 kHz.

3.3.3 Locking Signal

We were able to produce an error signal by modulating the frequency. The laser's optical frequency was modulated by the AOM by ±500 kHz at a rate of 100 Hz. Ideally, we would have modulated at a higher frequency, but we are limited by the bandwidth of our detection system. The fluorescence was collected by the PMT and demodulated using the lock-in amplifier to produce an error signal. The following plot shows the error signal which is the derivative corresponding to the fluorescence signal.

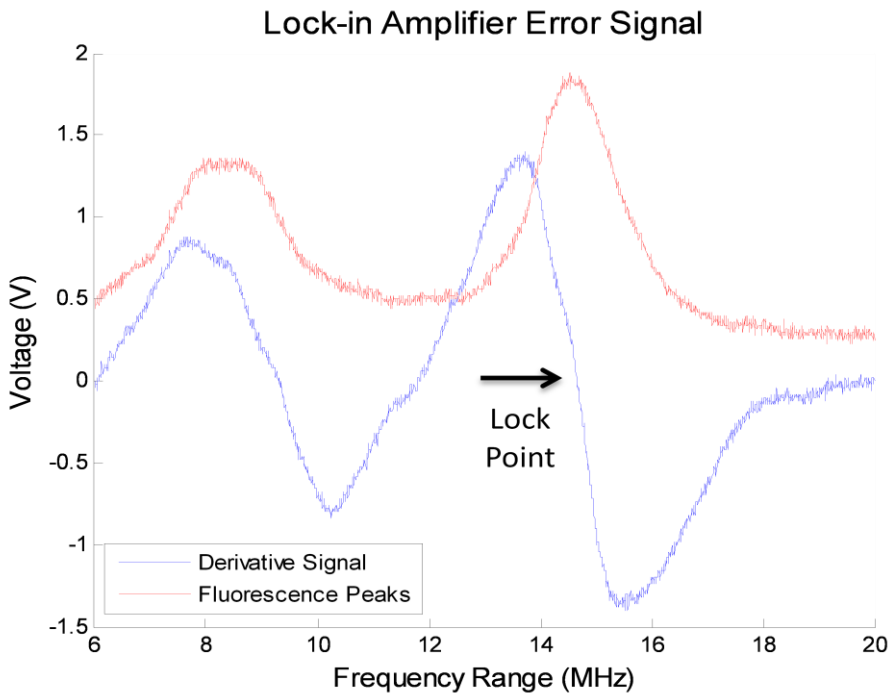

Figure 36 Derivative signal produced by lock-in amplifier from the fluorescence signal.

This error was fed into the feedback circuitry which allows us to lock to either an upwards or downwards sloping zero crossing. The control system feeds back onto the PZT and laser current to stabilize the frequency. By monitoring the fluctuations of the voltage signal, we can infer the accuracy and stability of the lock by using Figure 36. The frequency fluctuations are related to the voltage fluctuations by the inverse of the slope

at the zero crossing. Below is a plot showing the voltage fluctuations of the fluorescence signal due to the frequency fluctuations of the laser.

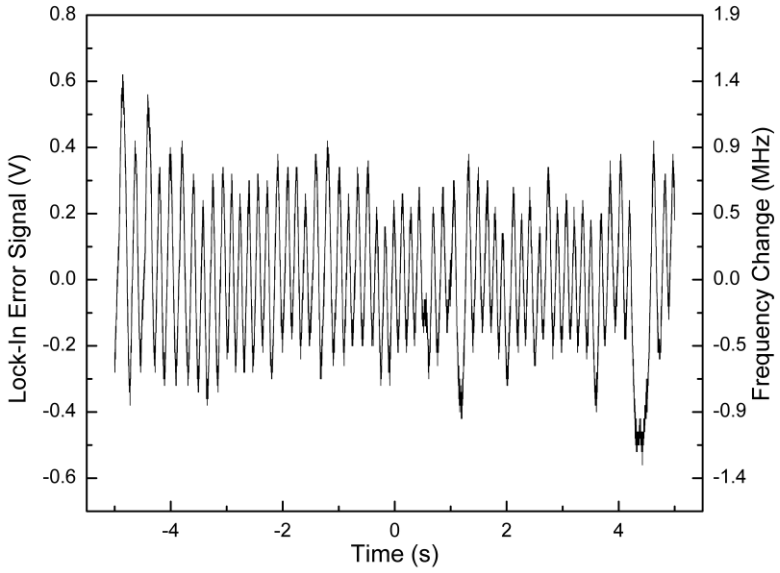

Figure 37 Voltage fluctuations of the PMT signal due to frequency excursions of the laser.

Based on the peak-to-peak voltage fluctuations of the signal in Figure 37, we calculated the frequency excursion of our lock to be approximately ±900 kHz of the atomic reference frequency.

3.3.4 The Effect of the Heating System on Hyperfine Structure

The magnetic field produced by the heating coils destroys the hyperfine structure of the atomic spectrum and makes it impossible to lock to the transition. Therefore, we have to heat the rubidium cell to the desired temperature (80°C), turn off the heating elements, and conduct our experiments.

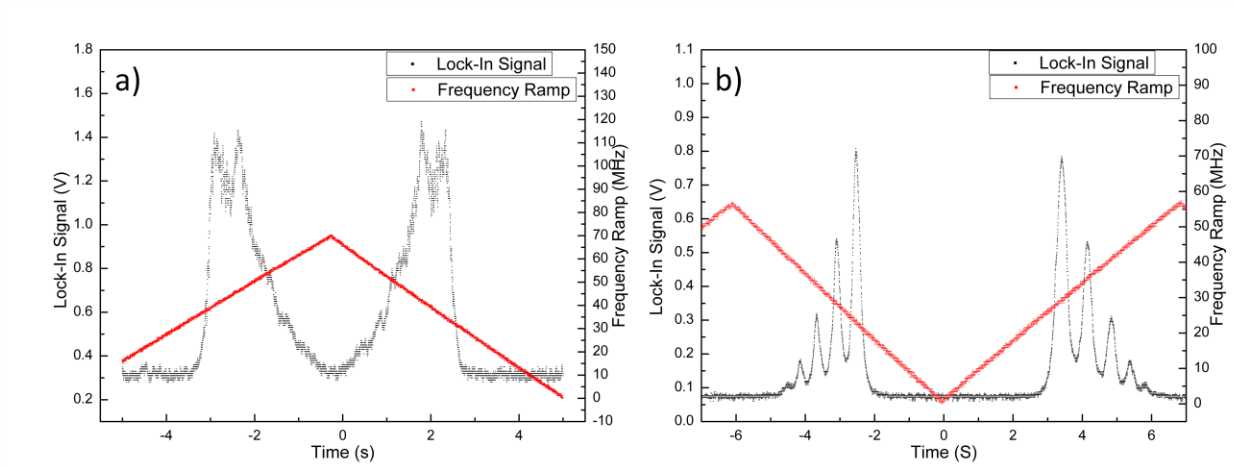

Figure 38 The heater distorts the emission spectrum due to the induced magnetic field. The red line shows the voltage of the PZT which scans the frequency range.

The sample typically stays warm for 10-20 minutes, but as it cools the density of the gas decreases, leading to a weaker signal. As the signal decreases, the slope of the zero crossing becomes less steep, which changes the error signal gain. This makes it difficult to properly tune the control system.

3.4 Conclusion

We were successful in stimulating the $5S_{1/2}$ - $5D_{5/2}$ two photon transition in rubidium. By modulating the frequency of the laser and then demodulating the resulting fluorescence, we were able to produce a frequency dependent error signal. Using this error signal we were able to lock our laser to within 1 MHz of the atomic reference frequency. This is an improvement over the unlocked laser which fluctuates by 20 MHz. However, this lock error needs to be significantly decreased for the stabilized laser to be used for the frequency comb. The two largest sources of locking error are the inability to properly tune the control system as the temperature is not stable and broadening of the peaks due to several experiment setup dependent factors. These factors include magnetic fields (both from the earth and electronically induced) and transit time broadening which we estimate to be approximately 300 kHz.

3.5 Recommendations

To improve the lock we recommend reducing the magnetic field induced by the heating coils. For the intended application of the laser for the frequency comb, the heating coils must be on while locking the laser. Lining the inside of the tube with mu-metal will block magnetic fields. Mu-metal is a nickel-iron alloy with high magnetic permeability. This provides a low reluctance path for magnetic flux leading to its use as magnetic shields

against static or slowly varying magnetic fields. If this does not work, alternative heating methods will have to be implemented. In particular, switching from AC current to DC current and increasing the resistance of the heating elements to limit current. By eliminating parasitic magnetic fields, we can keep the heating elements on while locking the laser. The constant temperature will stabilize our signal and allow for the gain of the feedback control system to be optimized to minimize frequency fluctuations.

The effects of beam power and transit time broadening must also be investigated. The focal lengths of the lens on either side of the oven can be varied and the AOM can control the power of the beam. The important parameter for signal strength is beam intensity, which is the ratio of the laser power to the beam's cross sectional area at the lens' focus. There is a trade off between SNR and broadening. A smaller beam width increases intensity and a hotter cell increases the absorption. Both of these factors lead to improved signal, but at the cost of a broader peak.

Finally, we recommend that a photomultiplier tube with a smaller output capacitance should be acquired. This will increase the bandwidth of the detection system and allow the lock-in amplifier to modulate the signal at higher frequencies. This will reduce the 1/f contribution to the noise and allow us to decrease our signal strength by broadening our beam.

4 Project Deliverables

4.1 List of Deliverables

Our original deliverables as outlined in the project proposal are listed below. However, our project has changed significantly in scope since the submission of the proposal. The first two items were abandoned in favour of the atomic transition lock outlined previously in this report. The third item is still relevant to this project and our locked laser has been demonstrated to be stable to within ±900 kHz when locked to an atomic transition of Rb.

1. Error signal electronics circuit
2. Functional PDH lock
3. Demonstration of laser stability

An updated list of deliverables with their current status is listed below:

1. Determination of laser linewidth by locking two lasers together – the two lasers have been locked to within 300 kHz, however in order to achieve a 10 kHz lock other methods need to be investigated.
2. Setup Rb atomic transition lock – an oven to house a Rb vapour cell, fluorescence collecting optics, and a PMT was designed and constructed. This oven and detection system was demonstrated to be capable of locking the laser to an atomic transition of Rb.
3. Demonstration of laser stability – the laser has been demonstrated to be stable to within 1.8 MHz of an atomic transition of Rb, however a tighter lock can be achieved by implementing simple changes to our setup.

4.2 Financial Summary

#	Description	Quantity	Vendor	Cost	Purchased by:	To be funded by:
1	Aluminum stock	1 kg	UBC PHAS	$30.00	Jon-Paul Sun	Project Sponsor
2	Polycarbonate	12” X 12” X ¼”	McMaster Carr	$42.74	Project Lab	Project Lab
3	LA1951-A Ø1” N-BK7 Plano-Covex Lens	1	Thorlabs	$31.80	Will Gunton	Project Sponsor
4	LCP02 30 mm to 60 mm Cage Plate Adapter	1	Thorlabs	$38.00	Will Gunton	Project Sponsor
5	Mu Metal	15” X 0.42” X 0.01”	McMaster Carr	$57.40	Will Gunton	Project Sponsor
6	ZMY-2+ Double Balanced Mixer	1	Minicircuits	$84.95	Will Gunton	Project Sponsor
7	SLP-10.7+ Low-Pass Filter	1	Minicircuits	$34.95	Will Gunton	Project Sponsor

4.3 Ongoing Commitments

A commitment to continue this project has been made by team members until the end of their tenure at UBC. Our future work will primarily focus on implementing the suggestions outlined in the recommendation section of the report on how to improve the frequency lock accuracy.

5 Recommendations

To achieve a tighter two-laser lock it is necessary to determine whether the lasers are limited to 300 kHz or if the signal to noise of the photodetector limited the result. Since we are able to control the centre frequency of our beatnote by tuning the PZT, we can use a photodetector with a lower bandwidth but higher resolution to measure the betnote width.

To improve on the rubidium lock we recommend implementing mu-metal shielding in the oven to dampen magnetic fields. The effects of power broadening and transit time broadening should also be investigated to optimize the beam waist and intensity in the vapour cell. A final recommendation for this setup would be to either acquire a new photomultiplier tube or modify the existing one to decrease the output capacitance. This would allow for higher modulation frequencies with the lock-in amplifier and reduce 1/f noise.

6 Appendices

A1 Intensity Fluctuations Filtering Circuit

The accuracy of the lock for stabilizing the laser's frequency is affected by intensity fluctuations of the lasers. The power fluctuations shift the zero crossing which cannot be distinguished from frequency fluctuations. Therefore, it is desirable to have a circuit which can filter out these power fluctuations. Below is the proposed circuit design to limit the system's sensitivity to intensity fluctuations. The design requires three steps: amplifying, clipping and filtering the input signal. The input to the circuit is a frequency signal with variable amplitude (Figure 1A).

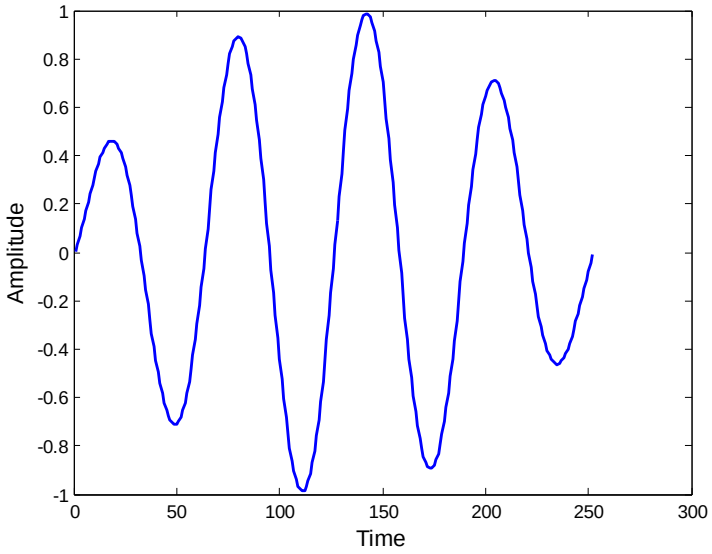

Figure A1 Variable amplitude sinusoid which is inputted into the circuit.

The signal is then amplified using a high-speed heterojunction bipolar transistor (HBT). This amplified signal is shown below.

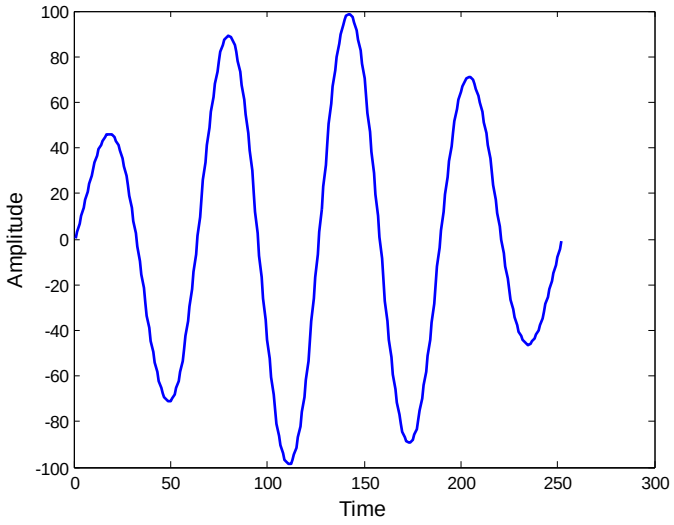

Figure A2 Amplified signal using an HBT

The signal is then clipped using a diode rectifier circuit to produce a square wave. The amplification step is needed so that the slope of the transitions is very steep. The amplitude of the square wave is determined by the diode cut off voltage.

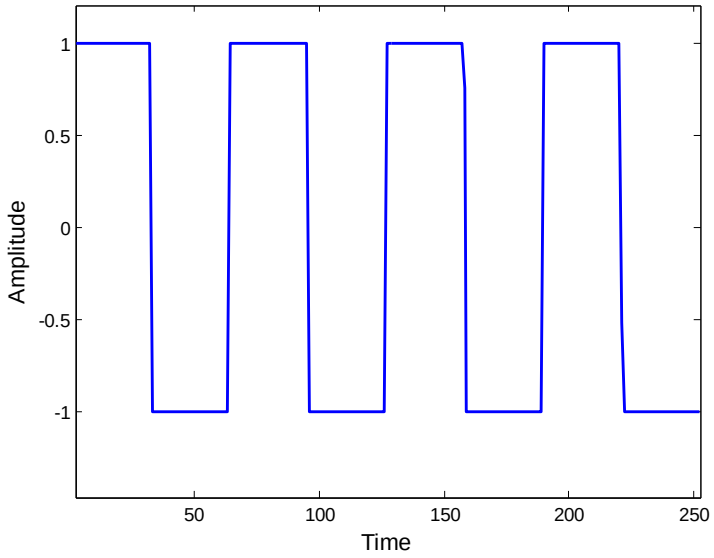

Figure A3 Clipped signal using a diode rectifier circuit.

The spectrum of the square wave is all odd harmonics of the frequency. This is shown in the following figure. If the spectrum is filtered to leave only the first harmonic, the resulting time domain signal is constant amplitude sinusoid.

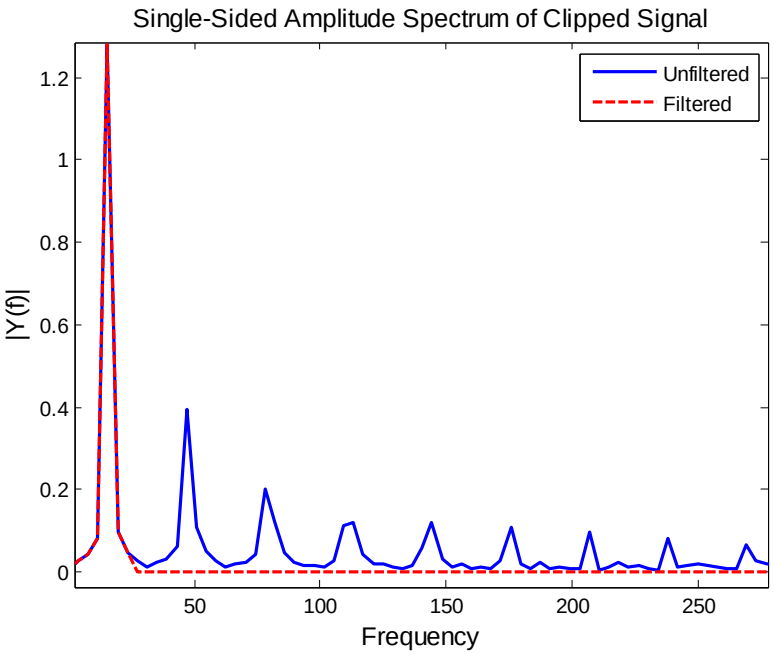

Figure A4 Filtered and unfiltered spectrum of the clipped signal.

After the filtering step, the resulting signal has the same frequency, but with a constant amplitude defined by the diode voltage.

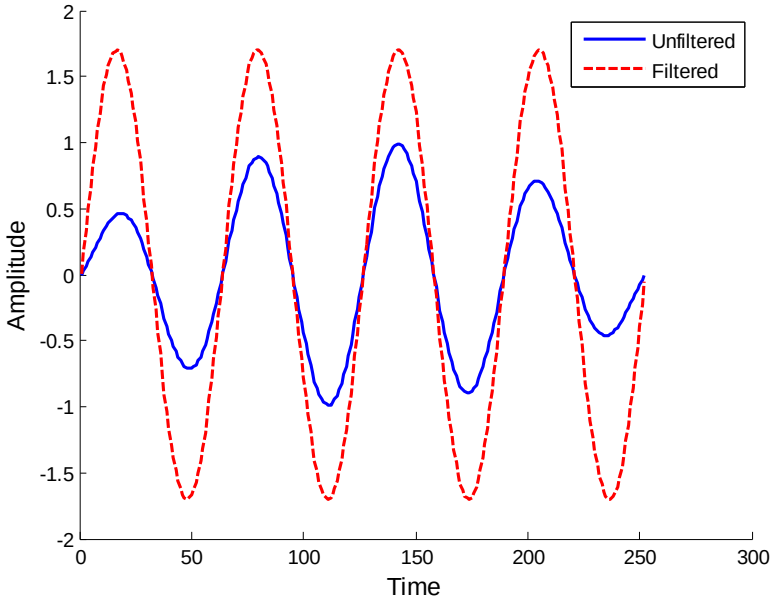

Figure A24 Original signal with variable amplitude and filtered signal with constant amplitude

The circuit schematic of this design is shown on the following page. The circuit consists of an HBT amplifier, two diodes for clipping the positive and negative voltage signals, and five 8th order Butterworth filters. The clipped signal is routed to one of the filters manually using two switching ports.

7 References

[1] W. Bowden, J. Sun, D. Quentin. "*Recommendation Report: Design and Characterization of ECDL"* (2011)

[2] F. Nez, F. Biraben, R. Felder and Y. Millerioux, Optics Communication, Vol. 102, 432 (1993).

[3] J. Ullrich *et al*, *Recoil-ion and electron momentum spectroscopy: reaction-microscopes"*, Rep. Prog. Phys., 66, 1463 (2003).

[4] K. Tao, "*Doppler-free Two-photon Spectroscopy."* Undergraduate Honors Thesis. UBC Physics Department.

[5] Jeff Hecht. PHOTONIC FRONTIERS: FREQUENCY COMBS. Online http://www.laserfocusworld.com/articles/print/volume-43/issue-6/features/photonic-frontiers-frequency-combs-frequency-combs-achieve-extreme-precision.html (2007)